AD

AMMRC CR 70-5 (F)

FEASIBILITY STUDY OF COLUMBIUM ALLOY CASTINGS

NOVEMBER 1971

R. J. BEAUREGARD
Avco Lycoming Division
Stratford, Connecticut 06497

FINAL REPORT — CONTRACT NUMBER DAAG46-69-C-0163

Prepared for

ARMY MATERIALS AND MECHANICS RESEARCH CENTER
Watertown, Massachusetts 02172

The findings in this report are not to be construed as an official Department of the Army position, unless so designated by other authorized documents.

Mention of any trade names or manufacturers in this report shall not be construed as advertising nor as an official indorsement or approval of such products or companies by the United States Government.

DISPOSITION INSTRUCTIONS

Destroy this report when it is no longer needed.
Do not return it to the originator.

Unclassified

Security Classification

DOCUMENT CONTROL DATA - R & D

(Security classification of title, body of abstract and indexing annotation must be entered when the overall report is classified)

1. ORIGINATING ACTIVITY (Corporate author) Avco Lycoming Division Stratford, Connecticut 06497	2a. REPORT SECURITY CLASSIFICATION Unclassified 2b. GROUP

3. REPORT TITLE

FEASIBILITY STUDY OF COLUMBIUM ALLOY CASTINGS

4. DESCRIPTIVE NOTES (Type of report and inclusive dates)

Final Report

5. AUTHOR(S) (First name, middle initial, last name)

R. J. Beauregard

6. REPORT DATE	7a. TOTAL NO. OF PAGES	7b. NO. OF REFS
November 1971	90	3

8a. CONTRACT OR GRANT NO.	9a. ORIGINATOR'S REPORT NUMBER(S)
DAAG46-69-C-0163 b. PROJECT NO AMCMS Code 4097.92.9.P6013 (X69) c. d.	AMMRC CR 70-5 (F) 9b. OTHER REPORT NO(S) (Any other numbers that may be assigned this report)

10. DISTRIBUTION STATEMENT

Approved for public release; distribution unlimited.

11. SUPPLEMENTARY NOTES	12. SPONSORING MILITARY ACTIVITY
Details of illustrations in this document may be better studied on microfiche	Air Materials and Mechanics Research Center Watertown, Massachusetts 02172

13. ABSTRACT

The objective of this program was to determine the feasibility of investment casting columbium alloys, namely, B-66 and C-3015. The REMET molding process, patented by REM Metals, Inc., Albany, Oregon, was used for the entire casting effort.

Multiple test specimens were fused silicide coated and subjected to stress-rupture, tensile, ballistic impact, and environmental testing. At 2200° F, the rupture strength of the cast alloys is much greater than the wrought form. Tensile strength and ductility of the alloys were unacceptably low for engineering applications. Silicide coatings showed visible signs of distress after 120 hours of testing.

The application of columbium alloys for investment casting appears promising; however, additional development is required to optimize molding and casting processes to the point where quality castings can be produced consistently.

DD FORM 1473 REPLACES DD FORM 1473, 1 JAN 64, WHICH IS OBSOLETE FOR ARMY USE

Unclassified

Security Classification

Security Classification

14 KEY WORDS	LINK A		LINK B		LINK C	
	ROLE	WT	ROLE	WT	ROLE	WT
Casting						
Niobium Alloy						
Properties Testing						
Refractory metal alloys						
Investment Castings						
Molding Techniques						

Unclassified

Security Classification

AMMRC CR 70-5(F)

FEASIBILITY STUDY OF COLUMBIUM ALLOY CASTINGS

R. J. BEAUREGARD

Avco Lycoming Division
Stratford, Connecticut 06497

NOVEMBER 1971

Final Report - Contract No. DAAG46-69-C-0163

AMCMS Code 4097.92.9 P6013 (X69)

Prepared for:

ARMY MATERIALS AND MECHANICS RESEARCH CENTER
Watertown, Massachusetts 02172

ABSTRACT

The objective of this program was to determine the feasibility of investment casting columbium alloys, namely, B-66 and C3015. The REMET molding process, patented by REM Metals, Inc., Albany, Oregon, was used for the entire casting effort.

Early in this program, it was necessary to establish the optimal mold design and preheat temperature. Two tungsten interface layers and maximum (capability) mold preheat were selected as the mold and casting parameters that would ensure the best fluidity consistent with a contamination-free surface. To improve the fill and soundness of cast parts by eliminating possible gas entrapment, the effect of venting the fluidity mold was investigated. However, other casting variables overshadowed the venting effect so no conclusive results were obtained.

After evaluating the effects of mold gating on specimen fill, molds containing multiple test specimens, such as threaded test bars, airfoil-shaped oxidation test paddles, and turbine nozzle vanes (both solid and cored) were cast. Although the fill and soundness of the cast specimens were erratic, there was no surface contamination. These specimens were fused silicide coated and subjected to tensile, stress-rupture, ballistic impact, and environmental testing.

Results of the stress-rupture testing conducted at 2200°F indicated that cast columbium alloys exhibited a twofold improvement in life over equivalent wrought columbium alloys. The tensile strength and ductility of the cast columbium alloys at both room and intermediate temperatures were unexpectedly low. Dynamic oxidation testing at an average metal temperature of 2200°F demonstrated that coated airfoil-shaped paddles of columbium alloy that had previously been damaged with ballistic impact were structurally intact after 120 hours of cyclic exposure.

The application of columbium alloys for investment casting of gas turbine engine components appears promising. But, before these alloys can be consistently cast into complex shapes, improvements in alloy fluidity and foundry practices will be required. Improved coating/alloy systems will also be required before the widespread introduction of cast columbium alloys into advanced gas turbine applications is possible.

FOREWORD

This report was prepared by the Avco Lycoming Division, Stratford, Connecticut under Army Contract G46-69-C-0163. The contract was administered under the direction of the U.S. Army Materials and Mechanics Research Center with Kenneth D. Holmes providing technical supervision.

This project has been accomplished as part of the U.S. Army Manufacturing and Technology Program, which has as its objective the timely establishment of manufacturing processes, techniques or equipment to insure the efficient production of current or future defense programs.

Richard Beauregard was the principle investigator in the program. The work was carried out under the direct supervision of Bruce A. Ewing, Chief of Materials Development. Overall program supervision was provided by W.R. Freeman, Jr., Director of Materials and Process Technology Laboratories Department. The author wishes to acknowledge the contributions of Gary Lane and especially Jeremy J. Walters for their efforts in the earlier stages of this program. Acknowledgement is also given to L. Fiedler for his valuable assistance in the writing of this final report and to Dallas Augustine who performed the environmental testing and analysis.

TABLE OF CONTENTS

LIST OF ILLUSTRATIONS

LIST OF ILLUSTRATIONS

LIST OF TABLES

I. INTRODUCTION

One of the most effective means of increasing the overall performance of a gas turbine engine is to increase the turbine inlet temperature. Such increases have been accomplished primarily through the use of extensive internal cooling of blade and vane components. However, in small gas turbine engines, cooling techniques soon become limited because of miniaturization problems and reduced cycle efficiency associated with cooling air requirements. Although the high temperature capabilities of nickel- and cobalt-base alloys have been extended by protective aluminide coatings and composition modifications, their creep-rupture strength and the microstructural instability of both matrix and coating system generally limit metal temperatures to about 1800°F for blades and 1950°F for vanes.

The need for other materials having a higher temperature capability than those presently in use periodically focuses considerable attention on the refractory metals, i.e., columbium, molybdenum, tantalum, chromium, and tungsten. Although these latter metals possess high temperature strength generally acceptable for high-temperature turbine engine usage, their susceptibility to oxidation imposes severe limitations on their utility. Of the refractory metals, the more advanced, low-density alloy systems of columbium are the most attractive candidates for potential turbine applications. To date, much effort has been expended by turbine engine manufacturers and refractory metal producers to develop a columbium alloy capable of withstanding temperatures in excess of 2500°F. The principal disadvantage with columbium, however, is its poor oxidation resistance that necessitates a satisfactory protective coating system to permit successful gas turbine engine operation. Previous attempts to use columbium alloys in high temperature gas turbine applications were discouraging because of the lack of an adequate coating system. Today, however, there has been revived interest to introduce columbium alloys into advanced engine designs. Stimulus provided by improvements in protective coating systems culminated in an Air Force engine evaluation of wrought columbium alloy vanes and the reported development of alloy substrates exhibiting improved oxidation resistance.

In conjunction with recent improvement in applying protective coatings and columbium alloy development, technology in the investment casting of reactive materials also has advanced thus enhancing the promise for improved economy and design simplicity. In particular, recent product improvement work* with investment cast titanium has demonstrated that

*U. S. Army/Avco Lycoming Product Support and Component Improvement Program CY 1968/69 Quarterly and Final Report Nos. 3162.1/2/3/4 (Improved Compressor) and 4212.2/3 (Investment Cast Titanium Impeller)

complex configurations can be cast to finished dimensions having virtually no surface reaction with the molding material. The success of casting extremely reactive materials with high melting points, such as titanium alloys, is significant particularly when the concept is extended to refractory materials that are known to share a common degree of casting difficulty.

Since recent advances of this combined technology have been made in areas of protective coating systems for columbium alloys, development of oxidation-resistant columbium alloys and casting techniques for reactive metals, it is logical to consider using columbium for investment casting of gas turbine engine components. The successful implementation of these latest developments into the design of hot-sections for advanced gas turbine engines could result in significant improvement in both engine capability and efficiency. As a result of these latest advances in casting technology, a program was begun to investigate the feasibility of casting columbium alloys. The subject program centers around the use of the REMET molding process, since a suitable mold material is the key to the successful investment casting of any alloy system. Because of the limited nature of the effort, however, only those parameters that, at the onset, seemed most important to the mold process were investigated. Attempts to define and optimize all of the pertinent casting variables essential to the development of a production process were outside the scope of this investigation.

II. DEVELOPMENT PROGRAM

The development program plan originally provided for:

1. Selection of alloys and coatings
2. Evaluation of alloy fluidity
3. Evaluation of mold gating
4. Casting and coating test specimens
5. Testing of oxidation and mechanical properties

Initiation of each of these phases was contingent upon the successful completion of the preceding phase.

When it became evident during the fluidities evaluation that gas entrapment was possibly contributing to the poor fill and soundness of cast specimens, an effort to evaluate venting the fluidity mold was added to the program plan.

CASTING PROCESS

REM Metals Corporation of Albany, Oregon, was selected as the subcontractor for the entire casting effort. The basis for the selection of REM in this program was the successful performance of their patented REMET mold process in the casting of titanium alloys. Although they had no previous experience in casting columbium, it was felt that the high melting point and extremely reactive nature of columbium and titanium alloys were similar enough to warrant attempts at casting columbium alloys using the REMET mold process.

Basically, the selected mold process is a modification of the shell molding process. The important feature that minimizes surface reactivity when casting highly reactive alloys is the use of metallic tungsten layers at the mold/metal interface. To produce a mold, a wax pattern of the desired shape is dipped into a tungsten powder slurry to form the first layer. After a drying period, this coating process is repeated until the desired number of tungsten layers are built up. Backup layers of stabilized zirconia are then applied also by dipping to give the tungsten layers additional support. Following removal of the wax with a chlorinated solvent in an autoclave, the molds are baked at 500°F to drive off moisture and remove the last traces of wax and the chlorinated solvent. The molds are then cured in a hydrogen atmosphere at 2150°F followed by an anneal at 2400°F in vacuum. The molds are cooled under vacuum and removed from the furnace for use at a later time.

In conjunction with the REMET mold process, REM Metals uses a consumable-electrode vacuum casting furnace (Figure 1). Using this technique, the alloy to be cast is formed into an electrode either by welding small chunks of alloy together or by casting a round bar. To protect the water-cooled copper crucible from arc damage during subsequent melting, a skull is prepared, initially, by carefully melting chips of the same material in the crucible and then pouring the molten metal out. Due to the different rates of expansion, the skull of solidified alloy can be removed from the crucible and used for subsequent melts of the same alloy.

The furnace used in the REM process also allows for preheating of the mold prior to pouring. This is accomplished by keeping the mold in a preheat chamber until the melt has been made. The preheat chamber is an integral part of the casting furnace, being separated from it by a molybdenum sheet metal curtain that reflects heat back into the preheater. The mold is surrounded on the other three sides by heating elements. For temperature control, a thermocouple placed on the side of the mold

closest to the molybdenum curtain. Preheat capability in the REM furnace is limited to 1400°F.

ALLOY AND COATING SELECTION

The selection of the two columbium alloys, B-66 and C-3015, at the outset of this program was based on favorable reports related to oxidation resistance, availability, cost, coatability, and mechanical properties. The nominal compositions of these alloys are shown in Table I. The B-66 alloy, developed by Westinghouse, has been in existence for a number of years and has found application in its wrought form in a number of programs conducted by governmental agencies and the aerospace industry. This alloy is considered as having moderate strength with excellent coatability and good thermal fatigue strength. The C-3015, which is a relatively new alloy developed by Wah Chang Albany Corporation, was designed to have a combination of oxidation resistance and elevated temperature stress-rupture life superior to other commercially available columbium alloys.

The Sylvania R512E coating (iron-chromium-silicon) was selected as the most promising coating for the B-66 alloy based on published reports* and discussions with Sylvania. The Vac-Hyd VH112 coating (tantalum-iron-molybdenum-hafnium-chromium-silicon) was selected as the most promising coating for C-3015 based on discussions with Wah Chang Albany Corporation. In both cases, these coatings are of the fused silicide type. The R512E coating is applied in one step, the slurry being fused at 2580°F. The VH112 coating is applied in two steps with fusion temperatures of 2525°F and 2475°F.

FLUIDITY EVALUATION

The fluidity of any given metal being cast is dependent both on the superheat of the molten metal, i.e., that portion of the heat content available above the liquidus, and on the rate at which this heat is lost through the walls of the mold once pouring is initiated. Generally, the longer the metal remains molten in the mold during pouring, the better the fill and soundness of the cast part will be. Unfortunately, in the case of a reactive

*Hauser, H.A. and Holloway, Jr., J.F., "Evaluation and Improvement of Coatings for Columbium Alloy Gas Turbine Engine Components," Report AFML-TR-66-186, Pratt & Whitney Aircraft Division, United Aircraft Corporation, East Hartford, Connecticut, Contract AF #33(9615)-2117 (May 1968)

metal, a lengthy period in the molten state also increases the chances of surface contamination by increasing the time available for the molten metal to react with the mold material. Therefore, surface contamination was considered an important aspect of the fluidity evaluation for columbium alloys.

The principal variables affecting fluidity include pour temperature, mold thickness, and mold preheat temperature. With the consumable-electrode furnace, adjustment of the pour temperature is extremely limited. Once the required amount of metal has been melted, the pour must be made before excessive heat is lost through the water-cooled copper crucible. Therefore, owing to inherent equipment limitations, no attempts were planned to intentionally vary the pour temperature in this program. The effect of mold preheat and the thickness of tungsten interface layers, however, were investigated for their effect on fluidity; mold fill, soundness, and surface contamination were used as the criteria for the evaluation.

A multiple-section fluidity mold was chosen to evaluate the two variables. Selection of this type of mold was based on its potential ability to deliver maximum casting information with a minimum number of pours. The fluidity mold configuration (shown in Figure 2) consists of a series of flat "wings" of variable thickness attached to a tapered sprue, which in turn is attached to the pouring cup. The initial thickness of the four bottom wings was 0.060 inch with the remaining four wings being 0.030 inch. After the first three pours, the thicknesses were changed to allow better interpretation of alloy fluidity. The four bottom wings were increased to 0.080 inch, the two center wings to 0.060 inch thickness and the two top wings to 0.030 inch thickness. Using this fluidity mold, it was planned to vary the number of tungsten layers and the mold preheat temperature to achieve the best fluidity and to avoid surface contamination.

VENTING EVALUATION

During the fluidity evaluation, it became apparent that possible gas entrapment was contributing to poor soundness and fill. To evaluate the effect of venting, additional wax patterns that had vents running from opposing wings back to the pouring cup were prepared for additional pours (see Figure 3). Mold fill, soundness, and surface contamination again were used as the criteria to evaluate the effects of venting.

GATING EVALUATION

Prior to the casting of specimens for testing in the final phases of the

program, several pours involving both B-66 and C-3015 alloys were scheduled to evaluate the effect of various gating techniques. To minimize the development activity, it was decided to use a combination mold to cast the three types of test specimens, rather than develop a mold for each. Wax patterns for the standard tensile specimens and the oxidation/thermal fatigue test paddle are shown in Figure 4. The third specimen (see Figure 5) represented a typical turbine vane application where the high-temperature capabilities of columbium alloys might be considered. Since this vane has an air-cooled airfoil, development of a suitable core to produce the cooling passage was also required.

At this time in the program, combinations of end and center gating were evaluated for the various test specimens, as required, to obtain satisfactory fill and soundness. End gating normally is preferred because it minimizes the amount of cleanup required to produce a finished part. Where necessary to obtain the required fill, additional gating was added to the wax patterns. The pours in this evaluation were made in sequence so that modifications to the gating practice could be made on subsequent pours.

TEST SPECIMEN CASTING AND COATING

Using the best techniques evolved during the gating evaluation, thirteen pours were planned to produce test bars, paddles, and vanes for use in later phases of the program. After casting and cleaning the specimens, REM returned them to Lycoming where the gates were removed. The specimens then were radiographed to determine their soundness. Bars and paddles deemed sufficiently sound for test received protective coatings. In general, the C-3015 specimens were coated with Vac-Hyd VH112, while the B-66 specimens were coated with Sylvania R512E. One paddle of each alloy was also coated with the opposite coating to investigate the relative effectiveness of the coatings on the oxidation resistance of the two alloys. Because the Sylvania R512E coated C-3015 paddle fractured during test setup, the R512E/C-3015 combination was not tested.

A chemical analysis was performed on each pour to detect any unanticipated variations in chemistry. Other test methods including metallography and microhardness were conducted as appropriate.

OXIDATION AND MECHANICAL PROPERTIES TESTING

Stress-Rupture Testing

Stress-rupture testing in air at 2200°F was performed by Metcut Research

Associates, Cincinnati, Ohio. The method of heating the coated columbium test bars is shown in Figure 6. A radiant heating tube of platinum was used to produce the 2200°F specimen temperature. The platinum tube was surrounded on the outside by insulation and a Hastelloy-X shield to minimize heat losses. The controlling thermocouple was attached directly to the platinum heating element. Recording thermocouples were fastened to the pull-bar system and had their tips bent over to lightly contact the coated test bar. This was done to minimize any possible reaction between the coating and the platinum-platinum 10% rhodium thermocouple. The high current required for resistance-heating the platinum tube was supplied by a transformer that was regulated by a temperature controller.

Earlier attempts to heat the bars by induction failed because the susceptor materials (Hastelloy-X and the zirconium diboride) were unable to withstand the temperatures. The first attempts at resistance-heating were with Hastelloy-X heating elements that proved to be unstable at 2200°F and, therefore, not reliable.

A total of twelve specimens, six of each alloy, were stress-rupture tested. Stresses of 10 to 20 ksi were used to test the B-66, while the C-3015 was tested at stresses of 20 to 32 ksi.

Tensile Testing

The remaining coated test bars were tensile-tested in air at Avco Lycoming on a standard Instron Model TT-C tensile machine. Tests were run at both ambient temperature and 1400°F. In both cases, a constant crosshead speed of 0.05 inch/minute was used.

Environmental Rig Testing

The materials evaluated in the oxidation test were Sylvania R512E coated and Vac-Hyd VH112 coated B-66 alloy; and Vac-Hyd VH112 coated C-3015 alloy. Specimens of Avco Lycoming 701 coated Inco 713C and M3608 nickel base alloys and Chromalloy SAC coated MAR-M-302 cobalt base alloy were included for comparison (for compositions, refer to Table I) as they represented alloys used for turbine blade and vane applications. By including these materials it was anticipated that the advantages peculiar to columbium alloys in such applications would be demonstrated. Table II includes a listing of these test specimens. The test specimens were in the form of airfoil paddles (Figure 7) cast as part of this program.

Because of the potential for catastrophic oxidation after a break in the protective coating, such as might occur during engine operation, it was decided to test some specimens with the coating intentionally damaged prior to the test.

Therefore, paddle specimens of Sylvania R512E coated B-66 and Vac-Hyd VH112 coated C-3015 were impacted in a ballistic impact rig (Figure 8). Specimens were held at a temperature of 2200°F and impacted (hot) on the convex surface using a 0.75 gram iron projectile with a velocity of 900 feet per second. Figure 9 illustrates the appearance of the impacted Sylvania coated B-66 specimen showing the impact area (arrow) and a nearby oxidized coating crack. Several attempts were made to impact coated paddles of C-3015; however, the projectile velocity that was sufficient to damage the coating caused the paddle to fracture (Figure 10), reflecting the poor impact resistance of the alloy. Consequently, coating damage had to be induced by using a deburring tool (Figure 11) to cut through the coating. Figure 12 shows the coated columbium alloys prior to cyclic oxidation testing.

Dynamic oxidation testing was conducted on a rig simulating the important environmental aspects of a gas turbine. In this test, the specimens are mounted in a holder fabricated of cobalt alloy L605 and locked into place with dowel pins of the same material. This attachment scheme is shown in Figure 13. The holder is then cycled in front of the hot products of combustion produced by an aircraft type combustor (Figure 14). Specimens were held at an optically determined peak specimen temperature of 2200°F for 2 minutes and then withdrawn into a cooling chamber to be cooled in still air for 1 minute. The fuel used was JP-4R (0.2 w/o sulfur). During the test, specimen temperature was measured with an optical pyrometer, which was later corroborated by an investigation with temperature indicating paints. Isotherms generated as a result of this latter investigation (Figure 15) revealed the peak temperature at the lower trailing edge location to be 2300°F, while the average peak metal temperature along the trailing edge was 2250°F.

Creep of the holder material upon exposure to the high temperature of this test unfortunately prevented the release of the test paddles from the holder without damage for periodic weight loss measurement. Consequently, the test was documented photographically at 20-hour intervals. Cyclic high-temperature oxidation testing of coated columbium and superalloy paddles was continued for 120 hours. At this time, coating failure and loss of mechanical integrity were noted for the coated superalloys remaining in the test. Coating distress was noted on all the coated columbium alloys. At this point, the paddles were freed mechanically

from the holder and examined metallographically to determine the extent of coating distress and base metal attack.

III. DISCUSSION

PRELIMINARY CASTING ACTIVITY

Skulls of the B-66 and C-3015 alloys were prepared prior to beginning the planned casting activity. Since in the making of initial skulls, a full crucible of metal must be melted, REM poured a cluster of four test bars from each alloy while their respective skulls were being prepared. This provided additional information to use in preparing the pour program. Both pours were made into molds having three tungsten layers and with no mold preheating since it was felt that no preheating and multiple tungsten layers would offer a reasonable chance of avoiding surface contamination. Subsequent molds would incorporate additional tungsten layers if contamination was evidenced, or increased mold temperature if no contamination was seen. The ultimate aim was to obtain the best fluidity with the least amount of contamination. For both B-66 and C-3015, good fill was obtained with the four-bar cast clusters and there was no vital indication of surface contamination.

FLUIDITY EVALUATION

To provide a quantitative means of evaluating the castings, the individual fluidity wings were removed, photographed, and radiographed. Fluidity was measured for each wing, as shown in Figure 16, and the wings were summed to provide a total "fluidity number" for each casting. A "porosity count" for each wing was made by counting individual pores noted in the radiograph plate. A summary of these data for both alloys is given in Table III. Fluidity castings were made concurrently for both alloys; however, discussions of detail results will be given separately for each of the alloys in subsequent paragraphs.

For the portion of the fluidity study involving preheated molds, it was intended to use preheat temperatures of 1000°F and 1500°F, the latter representing the maximum of the preheater. Above 1000°F, however, preheater control was inadequate. As a result, the temperature actually attained in the mold varied from 1150°F to 1400°F. The actual preheat temperatures monitored for fluidity molds are presented in subsequent paragraphs. Following the fluidity study, the preheater was reworked to hold constant at 1400°F, which was the target temperature for the remaining program pours.

Fluidity Evaluation of B-66 Alloy

Since good fluidity was exhibited by the test bar castings described above, it was decided to begin the fluidity study by pouring two fluidity castings using the same mold variables, i.e., three tungsten layers and no mold preheat. Figure 17 and Table III show the poor fluidity typically exhibited by these unheated molds. In addition to the poor fluidity shown by the casting produced in three-layer molds, apparent surface contamination was noted by metallographic examination.

The next two pours were made into unheated molds having four layer tungsten in the belief that the extra tungsten layer would eliminate the surface contamination. The fluidity of these two castings (Table III) was not impaired with respect to the three-layer castings, but the apparent surface contamination was still present.

A decision then was made to investigate two tungsten layers to determine if the thickness of tungsten substantially affected the amount of contamination. The first casting to be poured into an unheated mold was subject to a mold breakage problem, and the entire casting was contaminated. The replacement casting exhibited good fill and no contamination. In fact, further investigation revealed that the apparent surface contamination (Figure 18) shown by castings from previous three- and four-layer molds was caused by staining of the microstructure during sample preparation. Immediate observation of the surface microstructure of these samples following repolishing and etching revealed no discernible contamination (See Figure 18). This conclusion was substantiated by the results of microhardness traverses (Figure 19), which detected no surface contamination as revealed by an essentially constant level of hardness.

Since no surface contamination was detected on any B-66 pour, it was decided to begin the investigation of the effect of mold preheat on fluidity and surface contamination using a two-layer mold. Figure 17 shows a B-66 fluidity casting from a two-layer mold, preheated to 1160°F. The fluidity of this casting was better than the previous B-66 castings, as indicated in Table III. Again, there was no detectable surface contamination. Based on these encouraging results and similar results developed concurrently for C-3015 fluidity castings, additional B-66 fluidity evaluation was not considered necessary, and the remaining B-66 pours in the program were devoted to the production of test specimens.

Using a Leco Oxygen Analyzer, oxygen analyses were performed on random quantities of chips machined from fluidity wings or adjacent sprue material. The oxygen content of the B-66 fluidity castings ranged from 284 to 611 ppm (Table IV) and did not show a trend, with respect to interface layers. As the oxygen content of the single preheated mold casting fell between these values (i.e., 351 ppm), there was no apparent effect

of preheating on overall oxygen content, although the oxygen variation experienced was higher than anticipated. The problem of oxygen variation persisted throughout the program. Although the source of this variation was never identified, it was believed to be the result of either an inadequate furnace atmosphere or mold decomposition.

In summary, two layers of tungsten on the mold interface were adequate to protect against surface contamination for the preheat and metal superheats investigated. The effect of surface layer thickness on fluidity could not be assessed accurately due to poor fluidity with unheated molds. Limited preheating of a two-layer mold, however, resulted in nearly a fourfold increase in fluidity over the other conditions investigated and produced no surface contamination.

Fluidity Evaluation of C-3015 Alloy

As good fluidity was apparent by the C-3015 test bar casting produced during the preliminary casting effort, the fluidity investigation was initiated with the same mold variables, i.e., three tungsten layers and no mold preheat. Accordingly, one C-3015 fluidity casting (Figure 20) was poured under these conditions. The individual fluidity wings were removed, photographed, and radiographed, and analyzed. From the results shown in Table III, it can be seen that the fluidity of this casting was rather poor. The surface microstructure of the casting was free of apparent surface contamination (Figure 21). Since no surface contamination was detected using a three-layer unheated mold, it was decided to investigate the effect of mold preheat on fluidity and contamination at the three-tungsten layer level.

Two castings then were made with three-layer molds preheated to 1150°F and 1400°F, respectively. From the fluidity measurements presented in Table III, it can be seen that little improvement in fluidity was obtained by preheating the three-tungsten layer molds. Preheating the mold, however, did not lead to increased surface contamination. A decision was then made to reduce the number of tungsten layers from three to two to determine if better fluidity could be obtained. These two-layer molds were then preheated to provide a direct comparison with the preheated three-layer molds. Two C-3015 fluidity castings were poured into the two-tungsten layer molds preheated to 1000°F. The fluidity exhibited by using two-layer molds was much better than that obtained with the three-layer molds that had been heated to a slightly higher temperature (1150°F), as shown in Table III. A metallographic examination revealed no surface contamination.

Based upon these encouraging results, the next C-3015 casting (Figure 20) was poured into a two-layer mold heated to 1400°F. As shown in Table III, fluidity improved, and there was no evidence of surface contamination based on microstructure. The last pour in this phase of the program was made into a one-layer mold preheated to 1300°F since a trend appeared to be developing where fluidity increased as tungsten interface thickness decreased. Table III indicates that this casting exhibited good fill, and that there was no evidence of contamination. Microhardness surveys conducted to verify surface contamination results (Figure 22) showed no significant increases in hardness at the surface for all C-3015 pours except for one pour using a two-layer, 1000°F preheated mold. However, as three other pours made under equal, or more severe, conditions with respect to tungsten thickness and mold preheat did not show an increase in hardness, it was concluded that no trend was present regarding surface contamination and mold variables.

The results of oxygen analyses on C-3015 fluidity castings (Table IV) ranged from 103 to 293 ppm, with the single unheated mold casting (159 ppm) falling midway in the range. The casting obtained from the single tungsten layer mold had the highest oxygen content; however, there was no significant difference between two-and three-layer mold castings. Again, the variation in data may have overshadowed the effects of mold parameters.

To take advantage of an apparent similarity in casting behavior of the two alloys, the casting results for B-66 and C-3015 were combined to make the three-dimensional plot shown in Figure 23. In this graph, the fluidity measurements of both alloys were combined and plotted versus mold preheat temperature and number of tungsten layers. The combining of both alloys appears valid from the smoothness of the curve and yields more information than can be gained by considering each alloy individually. The plot indicates that optimum fluidity was obtained when the minimum number of tungsten interface layers and maximum mold preheat temperature are used. Current mold preheat temperatures at REM are limited to 1400°F maximum, although better fluidity probably would be obtained by preheating to a higher temperature. The optimum fluidity appeared to level off between two and one tungsten layers so that either was considered acceptable. Although no surface contamination (as determined by microhardness surveys and microstructure) was noted on any of the fluidity castings, it was felt that two tungsten layers would provide a better safety margin from unanticipated contamination. From these results, the casting variables selected as the best obtainable within the limitations of equipment capabilities were two tungsten interface layers and a mold preheat of 1400°F. These casting conditions were used

throughout the remainder of the program.

VENTING EVALUATION

As discussed previously, because of the evidence of gas porosity in the fluidity castings made when the casting effort began (Table III), a departure from the original program plan was made to investigate this phenomenon. It was felt that providing vents through which the gas could escape from the wings of the fluidity specimen might eliminate the porosity. By venting opposing wings, it was felt that each casting would be capable of individual analysis on the effect of venting, so both a B-66 and C-3015 vented fluidity casting (see Figure 3 for mold configuration) were poured. Unfortunately, however, the C-3015 casting disintegrated during cleaning because the caustic cleaning solution used to remove mold material from this casting was different from the one normally used; failure was attributed to the solution's being too reactive. Another C-3015 vented casting was poured. Because of the poor fluidity results obtained with the two intact castings, the effect of venting to eliminate gas porosity was not decisive.

Metallographic examination (Figure 24) and wet chemical analysis performed on the B-66 castings to determine the reason for the poor fluidity showed that the melting stock had been contaminated by stainless steel. The pieces of B-66 that are welded to form the electrode apparently had a piece of stainless steel inadvertently mixed with it. Further checking by REM revealed the presence of Permalloy and tungsten mixed in with the remaining B-66 chunks. Although contamination of the alloy could explain the poor fluidity in the B-66 casting, there was no obvious explanation for the poor fluidity in the C-3015 casting. Because of these results, it could only be concluded that the influence of venting, while apparently minor, was overshadowed by other casting variables and, therefore, was inconclusive. Since further evaluation was not within the scope of this program, further work in the area of venting was cancelled as none of the remaining scheduled pours could be spared if sufficient test specimens were to be cast.

GATING EVALUATION

The intent of this phase in the program was to evaluate the effect of different gating techniques on the quality of cast test specimens. The first series of gates evaluated are shown in Figure 25. The mold consisted of two test bars, two oxidation paddles, and one solid nozzle vane (REM had not developed a suitable core for columbium casting at this time). The test bars were gated at both ends and at the center. The paddles

were gated on the shank and on the end of the airfoil. The vane was gated across the leading edge. As mentioned previously, this mold and all subsequent molds employed two tungsten interface layers and maximum mold preheat (1400°F). A closeup of the cast details in C-3015 is shown in Figure 26. It is seen that there was poor fill in the paddles but comparatively better fill in the test bars and the vanes.

The second series of gates to be evaluated consisted of one test bar, end-gated only, and one test bar gated at both end and center. In both cases, the end gates were enlarged. The two paddles were end-gated as well as leading edge gated with both end gates enlarged. No change was made in the vane gating. As several previous pours in this program had resulted in mold breakage, the tungsten binder for the second stage configuration mold was changed in an effort to increase mold strength. However, the C-3015 casting that was poured using this mold failed to clean up and broke during cleaning. Apparently, when the binder decomposed, it released oxygen to produce an exothermic reaction that oxidized the surface, as shown in Figure 27 and fused the tungsten to the oxidized surface. Although the test specimens exhibited good fill, further gating investigations were conducted to determine if the exothermic reaction could have possibly contributed to the good fill.

Subsequent attempts to improve mold strength by changing the backup layers from zirconia to alumina also failed. Adequate mold strength finally was attained during the next mold making process by carefully incorporating support wiring of the specimens and using the normal tungsten binder and zirconia backup layers.

The third series of gates (actually two configurations) to be evaluated is shown in Figure 28. The gates were staggered vertically as they came off the sprue. The vane had a tapered gate in both configurations. All test bars were both end and center-gated. Three paddle gating arrangements (in two different molds) were also tried. Two paddles were gated on both ends, and a center gate placed on the flat of the airfoil. One paddle was full-gated on both the shank and the leading edge. The remaining paddle was full-gated on both ends and the leading edge. One configuration was cast in B-66, the other in C-3015. Radiographs showed the test bars to be sound, and although the threads were not completely filled, they were judged sufficient for test purposes. The paddle with full gates on both ends and the leading edge was not filled out, although the same configuration with only one end gate was filled out. The two identically gated paddles were completely filled; but removal of the center gate (not shown in the figures) presented a difficult task. For this reason, the paddle with gates on the shank and leading edge was considered as most

desirable. Both nozzle vanes (still solid) showed only slightly unfilled trailing edges. It was decided to use the same gating on future nozzle pours except for a flash of wax that would be added to the trailing edge of the pattern to aid in filling.

TEST SPECIMEN CASTING

After selecting the best gating techniques, only thirteen pours remained with which to accomplish the balance of the program. It was decided to pour six castings, three from each alloy, using the defined gating techniques and to analyze the yield of test specimens to determine which alloys and specimens to cast for the remaining seven pours. Two of the original six pours incorporated cored turbine vane waxes developed by REM. These cores were essentially the same as the REMET molds; i.e., tungsten-interfaced zirconia. The only difference was that they were made by coating the inside of a hollow pattern instead of the outside of a solid pattern as in mold making. One of the cored turbine vanes was filled completely, as shown in detail in Figure 29.

Of the remaining seven molds to be cast, two were leftover molds from the gating development portion of the program, and five were newly made molds. On the new molds, the center gate on the test bar was eliminated to make the gate removal operation easier, and the quantities of the different test specimens were adjusted to suit the testing phase of this program. All vanes on the new molds were cored.

Of the seven molds, four were poured with C-3015 alloy and three with B-66 alloy. There was a wide variation in the thread fill on the test bars. Also, none of the cored turbine vanes obtained from these pours filled out. In general, the fluidity of these last seven pours was considerably worse than the previous six pours; this can only be attributed to casting variables, which, at this time, were not controlled adequately. After the gates were removed, the individual test specimens were radiographed. None of the test bars exhibited any sign of porosity or shrinkage in the gauge area, although the paddles and vanes showed considerable porosity. Figure 30 shows typical test specimens of cast columbium that were produced during this program.

Microstructural Examination

In general, grain sizes in the columbium alloy castings were found to be a function of cross-sectional thickness. The coarsest grain sizes (ASTM 2 to 6) were found in sprue sections with test bar cross sections being finer (ASTM 5 to 7). Finest grain sizes were observed in fluidity

wings which were ASTM 6 to 8.

By comparison with the grain sizes typically found in superalloy castings, these grain sizes were much finer, reflecting the relative inability of the REM casting process (i.e., metal superheat and/or mold preheat) to retain heat within the mold during solidification.

Examination of representative as-cast B-66 specimens with the light microscope (Figure 18) revealed equiaxed grains of what appears to be essentially a solid solution. Examination of the microstructure with the electron microscope, however, revealed the presence of a second phase occurring as a fine dispersion throughout the matrix and in a massive form at grain boundary intersections and, less frequently, along the boundaries (Figure 31). X-ray diffraction analysis was performed on the residue left after electrolytic extraction of a typical sample of B-66. As shown in Table V, the only second phase that was observed in the sample was zirconium dioxide, ZrO_2. An excellent correlation was obtained between the observed d-spacings and the d-spacings of ZrO_2 given in the ASTM card file (card Number 13-307).

Examination of the C-3015 alloy with the ligh microscope generally revealed a structure that was finer grained than B-66 and quite heavily decorated with second phase precipitate as shown in Figure 21. The rod-like precipitate was semi-continuous along the grain boundaries, less frequent within a grain. Examination of the microstructure with the electron microscope more clearly shows the nature of this precipitate (Figure 32). A roughening of the matrix is also seen in Figure 32, but no evidence could be found to verify the existence of the apparent finely dispersed second phase. Table VI shows the data obtained by x-ray diffraction of electrolytically extracted particles typically present in cast C-3015 alloy. The residue was identified as being face-centered cubic with a lattice parameter of a =4.57 (calculated from observed d-spacings). Since the structure fits the MC type of carbide, x-ray fluorescent analysis was performed. The results indicated that the precipitates were high in hafnium and somewhat lower in columbium with a small amount of tungsten present. A literature search* revealed the existence of a complex carbide (Hf, Cb) C with lattice parameters between HFC (a_o = 4.63) and CbC (a_o = 4.47). Since the observed lattice parameter was intermediate between that of HfC and CbC and both hafnium and columbium were identified by fluorescent analysis, it is believed that the precipitate is a complex carbide consisting of a solid solution of HfC, CbC, and MC. The MC carbide designation is used to represent the possibility of tungsten or some other element being present as a carbide in the solution.

*Pearson, W.B., A Handbook of Lattice Spacings and Structures of Metals and Alloys, Vol. 2, p. 1347

STRESS-RUPTURE TESTING

Table VII and Figures 33 and 34 present the results of stress-rupture testing (in air) of cast and coated columbium alloys at 2200°F. For comparison, uncoated wrought columbium data (tested in vacuum) obtained from Wah Chang Albany Corporation show that both cast B-66 and C-3015 are significantly stronger than their wrought counterparts at 2200°F, and that cast C-3015 maintains a 2:1 strength advantage over cast B-66 (stress for 1000-hour life). However, the relatively low ductility of cast C-3015 suggests problems with high temperature brittleness.

TENSILE TESTING

Table VIII provides the tensile test results generated in this program with the cast columbium alloys. All tensile testing was performed in air on coated test bars (B-66/R512E and C-3015/VH112). As seen in Table VIII, the room temperature tensile strength and ductility of cast B-66 and C-3015 are considerably lower than for equivalent wrought material. Also, the cast material did not exhibit a yield point. At 1400°F, the tensile strength and ductility of the cast material was again considerably lower than equivalent wrought material, although the cast B-66 bars did exhibit a yield point.

When comparing cast tensile properties to wrought tensile properties for the same material, it is not uncommon to see lower strength and ductility values for the cast material; this is generally due to the finer grain sizes and more homogeneous nature of wrought materials made possible by working. The low tensile properites developed in this testing, however, were lower than would have been expected due to alloy form only.

Macroscopic examination of the failed test bars revealed fracture surfaces that were typically brittle in appearance. There were no apparent casting defects that could be associated with the poor performance of the test bars. Peculiar to all of these test bars, however, was the relatively high oxygen content, which was generally between 200 and 500 ppm (Table IV). For wrought columbium alloys, oxygen is normally under 200 ppm with specification limits normally set at 200 ppm and occasionally up to 300 ppm. Within the scope of this program, it was not possible to concluclusively establish oxygen as the prime contributor to the low ductilities. Prior experience with other columbium alloys, however, suggests that lower oxygen levels should be sought in future castings to minimize any tendency for lowering ductility.

The effect of silicide coating is another factor that might have contributed to the low tensile properties developed in these castings. Metallographic examination of as-coated specimens showed that the coatings contained cracks (Figure 35) that could have acted as notches. Coating cracks of this type, commonly found in refractory alloy coatings, are felt to be caused by differences in thermal expansion between substrate and coating. In order to determine whether or not the coating significantly influenced tensile properties, the R512E coating was machined off of a B-66 specimen that was then tensile tested at room temperature. As is indicated by Table VIII, the ultimate tensile and 0.2 percent yield strength of the machined bar was improved nearly twofold by comparison with coated test bar properties even though ductility remained below 1 percent as was the case with the coated specimens. This performance seems to verify the detrimental influence of the cracked coatings on tensile strength despite no improvement in ductility.

Overall, the disappointing tensile properties developed in this program dictate the need to improve the tensile properties of cast columbium alloy compositions. Improving the casting technique to the point where low oxygen contents can be consistently developed might be a major help in realizing this goal. An improved technique in itself, however, may not provide the final solution. Ultimately, compositions specifically tailored to the casting process will be required.

ENVIRONMENTAL RIG TESTING

Although coating evaluation was not a major part of the program, metallographic examination of representative samples before and after testing was conducted where possible. It was shown previously (Figure 35) that evidence of coating cracking was observed in both VH112 coated C-3015 and R512E coated B-66. In addition, sharp radii, e.g., paddle ends, had pronounced cracking as shown in Figure 36. It should be noted that these cracks were not seen when specimens were inspected by visual and fluorescent penetrant techniques. By contrast, the aluminide coatings applied to M3608, Inco 713C, and MAR-M-302 test specimens were free from apparent coating defects which is considered typical for these alloys. In general, the coating thicknesses were uniform from location-to-location with thicknesses ranging from 5.0 to 6.0 mils for columbium alloys.

Visual inspection of the coated columbium alloy paddles throughout the 120 hours of testing indicated differing degrees of coating degradation for each of the coating/substrate combinations. The C-3015 alloy paddles coated with Vac-Hyd VH112 were the only paddles on which apparent coating deterioration was not visually catastrophic for test periods up to 120 hours

(Figure 37). The coating on this paddle, however, showed minute blistering on the lower trailing edge (the hottest portion of the paddle) after 40 hours of testing. Throughout the remainder of the test, these blisters became larger and more numerous, eventually covering the length of the trailing edge. These blisters appear as the pebbled surface texture noted in Figure 37 (concave surface). At no point, however, did the blisters induce localized spalling.

Both the R512E and VH112 coatings spalled from the B-66 alloy during oxidation testing. No visible deterioration of the VH112 coating on B-66 was noted (Figure 38) during the first 60 hours of testing at 2200°F, but the inspection after 80 hours revealed small blisters along the entire trailing edge of the paddle where temperatures approach 2250°F. Spalling was observed along the trailing edge of the paddle after 100 hours of testing, and worsened during the remainder of the test.

The R512E coated B-66 showed blisters on the lower trailing edge after 40 hours of testing, at which time, it also was noted that a very fine scale was spalling from the paddle tip. This condition gradually worsened during continued exposure until after 100 hours of testing, spalling of the coating had begun to extend down the convex face of the paddle (Figure 39). At this point, the coating on the lower portion of the paddle was showing blisters and spalling of fine surface scale.

Ballistic impacting of the R512E coated B-66 paddle and manual damaging of the VH112 coated C-3015 paddle did not seem to impair the lives of these parts when exposed to dynamic oxidation testing (Figure 40 and 37, respectively). While these distressed areas were observed to locally oxidize during the course of the test, the lives of these parts were judged to be limited, not by this imposed distress, but rather by the general deterioration of the respective coatings.

Periodic observation of the coated superalloy paddles revealed deterioration of their coatings and the occurrence of substrate oxidation, expecially along the trailing edges. As would have been expected, the 701 coating on M3608 (Figure 41) broke down at the lower trailing edge and blistered after 60 hours of testing at paddle locations experiencing temperatures greater than 2200°F (the coating/matrix interface of this coating is known to melt at approximately 2175°F). After 80 hours of testing, cracks developed in the base material on the lower trailing edge where the coating had failed previously. During the remainder of the test, the cracks enlarged and degradation of the coating continued in the other locations.

The performance of coated Inco 713C (Figure 42) was generally poorer than that of coated M3608. Pronounced bowing of the Inco 713C paddles occurred after 40 hours and led to eventual removal of both specimens after 80 hours of testing. General blistering of the coating due to localized melting at the matrix/coating interface was observed early in the test, and deterioration of the entire trailing edge was evident after 40 hours of testing.

The MAR-M-302 paddle with Chromalloy SAC coating (Figure 43) also bowed but not to the degree experienced with Inco 713C. Spalling of the SAC coating occurred on the lower trailing edge after 40 hours of testing with significant substrate oxidation evident in this area after 60 hours. Inspection after 80 hours of testing revealed general coating deterioration over most of the paddle.

Microexamination of VHll2 coated C-3015, which appeared visually to be the least degraded specimen after 120 hours of testing, revealed substantial oxidation of the coating on the paddle. The local oxidation in the coating appeared to be associated with previously cracked areas (Figure 44), although it is reasonable that additional cracks occurred in the coating during testing. Although oxidation products filled the crack, this did not prevent oxygen from diffusing along these previously cracked paths. Substrate oxidation proceeded inward from these oxidized cracks and was more substantial on the trailing edge than in other locations (Figure 44). This increased oxidation is attributed to both the relatively sharp radius of the trailing edge, which aggravates the coating/matrix thermal expansion mismatch, and the higher temperature of the trailing edge of the paddle, which was 100° hotter than the leading edge (see Figure 15). Greater magnification of the substrate oxidation is shown in Figure 45. Transverse cracking at the coating and substrate interface and subsequent spalling were somewhat less in VHll2 coated C-3015 than in other specimens; this probably contributed to the better visual appearance of this coating and substrate combination.

Microexamination of VHll2 coated B-66 revealed that the oxidation of prior cracks and the linkup of these cracks resulted in spalling and the poor visual appearance of the coating. Coating cracks adjacent to areas where spalling eventually occurred along the trailing edge were more severely oxidized, and the network of linking cracks appeared more extensive than on the leading edge (Figure 46). When actual spalling of the coating occurred, oxidation of the B-66 substrate also was noted (Figure 47). Similar metallographic examination of R512E coated B-66 showed a linking of coating cracks at the interface of the diffusion zone and substrate (Figure 48).

After ballistically impacting an area of a B-66 paddle having R512E coating, cross-sectional examination revealed a predominantly transgranular crack network extending nearly through the paddle cross-section. Oxidation progressed inward within the confines of the ballistically impacted area. The coating adjacent to the impacted area was intact except for some cracking that was judged not unusual for this coating and substrate (Figure 49). There was no evidence of oxidation outside the ballistically impacted area.

As expected, metallographic analysis of the pack aluminide coated superalloys leaves no doubt that the useful lives of these coatings have been expended. In all cases, the coatings have broken up into islands of an aluminum-depleted, nickel-rich, solid solution (Figure 50), thus offering no further protection and providing a relatively free path for continued oxidation of the substrate.

In summary, environmental rig testing showed that coatings applied to the columbium alloy test specimens were incapable of affording complete protection over the 120 hours of testing performed at an average temperature of 2200°F. In spite of the coating distress developed, however, none of the columbium alloy test specimens showed signs of mechanical failure (buckling, bowing, cracking, etc.) as did the conventional superalloys. For short-life, high-performance gas turbine engines, the level of performance demonstrated by the columbium alloys may be adequate but, for high-performance engines that must be operated reliably for extended periods improved performance of the coating/alloy system will be required.

IV. CONCLUSIONS

Although the results obtained in attempting to investment-cast columbium alloys are promising, it is apparent that the equipment currently available and, perhaps, the techniques used are not sufficiently refined to enable consistent production of complex shapes. In general, it appears that further alloy and coating development is necessary if gas turbine components cast of columbium alloy are to be used.

Specific conclusions derived from this development program are:

1. The REMET molding process is capable of producing investment castings free of contamination in relatively complex shapes within the range of conditions investigated.

2. In general, decreasing the number of tungsten layers and increasing mold preheat temperature results in increasing fluidity.

3. At 2200°F, the rupture strengths of cast B-66 and C-3015 are much higher than the wrought form, with C-3015 being the stronger of the two.

4. The tensile strength and ductility of both columbium alloys were unacceptably low for engineering applications; this was possibly due to high oxygen content of the castings.

5. Impact resistance of the cast C-3015 test specimens subjected to ballistic impact testing at 2200°F was inadequate for gas turbine applications.

6. The silicide coatings applied to the cast columbium alloys exhibited visible signs of coating distress following 120 hours of testing. The intentionally distressed areas of coating did not accelerate coating/alloy degradation.

7. Resistance to oxidation at 2200°F will likely be the limiting factor in the use of cast columbium alloys. However, it should be noted that currently used high temperature alloys such as TD Nickel, TD Nichrome, IN853, NX188 (Nickel - 18 Molybdenum - 8 Aluminum) are also limited at 2200°F by their oxidation resistance in the uncoated condition.

V. RECOMMENDATIONS

Additional development effort is required to optimize the REMET molding and casting process to the point where quality castings can be produced consistently. Specific areas in this process requiring optimization and improvement are:

1. A redesign of the mold preheat system is imperative for any future columbium alloy casting because it is presently incapable of consistently reaching the high temperature desired for the casting of columbium alloys.

2. The introduction of superheat capability into the melting process may be desirable to further improve fluidity.

3. Improvements in the strength of the mold system would be beneficial in order to decrease mold breakage.

In general, consideration should be given to the possibilities of designing columbium alloys specifically for the investment casting process. With the availability of investment casting as a means of shaping metal, an entirely new approach to columbium alloy development is possible since use of the casting technique precludes the need for alloy hot-workability. With this added flexibility, it may be possible to formulate an alloy specifically for oxidation resistance and strength. Based on the demonstration of the creep-rupture advantages of compositionally similar cast forms over wrought forms, a review of previously investigated columbium alloys that may have exhibited interesting ductility and oxidation characteristics, but were low in hot strength, should be made.

TABLE I NOMINAL ALLOY COMPOSITIONS

	Weight Percent of Element													
Alloy	Hf	W	Ta	C	Zr	V	Mo	Cb	Cr	Co	Ti	Al	Ni	B
B-66	-	-	-	0.01	1.0	5.0	5.0	Bal	-	-	-	-	-	-
C-3015	29.0	16.0	1.0	0.1	1.5	-	-	Bal	-	-	-	-	-	-
M3608	-	-	7.25	0.15	0.1	-	2.7	-	10.0	10.0	1.25	6.0	Bal	0.015
INCO 713C	-	-	-	0.12	0.1	-	4.2	2.0	12.5	-	0.8	6.1	Bal	0.012
MAR-M-302	-	10.0	9.0	0.85	0.2		-	-	21.5	Bal.	-	-	-	0.005

TABLE II. TEST SPECIMENS USED FOR OXIDATION TESTING

Quantity	Alloy	Coating	Coating Damage
1	B-66	Sylvania R512E	Ballistically Impacted
1	C-3015	Vac-Hyd VH112	Manually Distressed
2	B-66	Sylvania R512E	None
1	B-66	Vac-Hyd VH112	None
2	C-3015	Vac-Hyd VH112	None
2	M3608	Lycoming 701	None
2	INCO 713C	Lycoming 701	None
1	MAR-M-302	Chromalloy SAC	None

TABLE III. FLUIDITY AND SOUNDNESS RESULTS FOR COLUMBIUM ALLOY FLUIDITY SPECIMENS

Alloy	Number of Tungsten Layers	Mold Preheat Temperature (°F)	Porosity* Count	Fluidity** (mm)	Comments
B-66	3	70	6	34	
B-66	3	70	7	3	Repeat of Previous Pour
B-66	4	70	13	50	
B-66	4	70	28	50	Repeat of Previous Pour
B-66	2	70	-	-	Mold Breakage Contaminated Pour
B-66	2	70	7	68	Repeat of Previous Pour
B-66	2	1160	13	221	Goal for Mold Preheat: 1500°F
C-3015	3	70	60	56	
C-3015	3	1150	25	58	Goal for Mold Preheat: 1500°F
C-3015	3	1400	90	45	Goal for Mold Preheat: 1500°F Repeat of Previous Pour Pouring Cup Broke and Fell into Molten Casting
C-3015	2	1000	60	203	
C-3015	2	1000	50	143	Repeat of Previous Pour
C-3015	2	1400	190	214	Goal for Mold Preheat: 1500°F
C-3015	1	1300	60	181	Goal for Mold Preheat: 1500°F

* Total count of pores on all wings.

** Measured as the axial length of completely filled wings, the lengths summed.

TABLE IV. OXYGEN CONTENT OF COLUMBIUM ALLOY CASTINGS

Alloy	Number of Tungsten Layers	Mold Preheat Temperature (°F)	Mold Type	Oxygen Content (ppm)
B-66	3	70	Fluidity	463
B-66	3	70	Fluidity	529
B-66	4	70	Fluidity	284
B-66	4	70	Fluidity	341
B-66	2	70	Fluidity	611
B-66	2	70	Fluidity	376
B-66	2	1160	Fluidity	351
C-3015	3	70	Fluidity	159
C-3015	3	1150	Fluidity	111
C-3015	3	1400	Fluidity	174
C-3015	2	1000	Fluidity	103
C-3015	2	1000	Fluidity	151
C-3015	2	1400	Fluidity	222
C-3015	1	1300	Fluidity	293
C-3015	2	1400	Vented Fluidity	194
B-66	2	1400	Vented Fluidity	307
C-3015	2	1400	Vented Fluidity	110
C-3015	2	1400	Gating Evaluation	195
C-3015	2	1400	Gating Evaluation	251
B-66	2	1400	Gating Evaluation	234
C-3015	2	1400	Gating Evaluation	284
C-3015	2	1400	Test Specimens	477
B-66	2	1400	Test Specimens	503
B-66	2	1400	Test Specimens	220
C-3015	2	1400	Test Specimens	228
B-66	2	1400	Test Specimens	244
C-3015	2	1400	Test Specimens	399
C-3015	2	1400	Test Specimens	417
C-3015	2	1400	Test Specimens	346
B-66	2	1400	Test Specimens	300
B-66	2	1400	Test Specimens	544
B-66	2	1400	Test Specimens	451
C-3015	2	1400	Test Specimens	501
B-66	2	1400	Test Specimens	426

TABLE V. X-RAY DIFFRACTION ANALYSIS OF EXTRACTED PHASES IN CAST B-66 ALLOY*

Observed d-Spacings	ZrO_2 d-Spacings ASTM Card No. 13-307
3.14	3.16
2.82	2.83
2.61	2.62
2.53	2.54
2.01	2.01
1.98	1.99
1.84	1.85
1.81	1.80
1.80	1.78
1.71	1.69
1.65	1.66
1.54	1.54
1.49	1.49
1.48	1.48
1.42	1.42

*Data obtained by Monochromatic $Cu K_\alpha$ Radiation, 45 kv, 35 ma

TABLE VI. X-RAY DIFFRACTION ANALYSIS OF EXTRACTED PHASES IN CAST C-3015 ALLOY*

Observed d-Spacings

2.64	1.38	1.05
2.30	1.32	1.03
1.62	1.15	

Calculated Lattice Parameter

face centered cubic

$a_o = 4.57$

Known Lattice Parameter

HfC: $a_o = 4.63$

CbC: $a_o = 4.47$

*Data obtained by Monochromatic $C_u k_\alpha$ Radiation, 45 kv, 35 ma

TABLE VII. 2200°F STRESS RUPTURE PROPERTIES OF CAST AND COATED COLUMBIUM ALLOYS

Alloy	Stress (Ksi)	Life (Hr)	Elong (%)	Comments
B-66	10	275.6	26	
B-66	15	181.9	-	Thread Failure. No Apparent Elongation.
B-66	16	79.6	14	
B-66	17.5	34.0	11	
B-66	19	18.9	10.5	
B-66	20	58	6	Less than 24 Hours at a Declining Temperature Due to Heating Element Malfunction.
C-3015	20	117.3	-	Broke on Unloading. No Apparent Elongation.
C-3015	22	222.1	<1	
C-3015	27	155.4	<1	
C-3015	29.5	211.7	-	Elongation Could Not Be Accurately Determined Due to Multiple Fractures.
C-3015	30	22.6	3.5	
C-3015	32	0.1	2.5	

TABLE VIII. TENSILE PROPERTIES OF CAST AND COATED COLUMBIUM ALLOYS

Alloy	Test Temperature					
	80°F			1400°F		
	UTS (psi)	0.2% Y.S. (psi)	Elong (%)	UTS (psi)	0.2% Y.S. (psi)	Elong (%)
Wrought B-66 *	115,500	95,000	20	98,800	66,000	16
B-66	62,750	No Yield	<2.0	53,000	44,500	<1.0
B-66	49,800	No Yield	<2.0	57,200	50,900	<1.0
B-66	52,100	No Yield	<1.0	56,800	47,000	<1.0
B-66	48,100	No Yield	<1.0	-	-	-
B-66 **	74,600	73,400	<1.0	-	-	-
Wrought C-3015 ***	112,000	119,000	4	114,000	78,300	9
C-3015	41,700	No Yield	<1.0	55,000	No Yield	<1.0

* Westinghouse Special Technical Data 52-364

** Coating Machined off Prior to Test

*** Wah Chang Data on Ht # 590060 Annealed at 3200°F

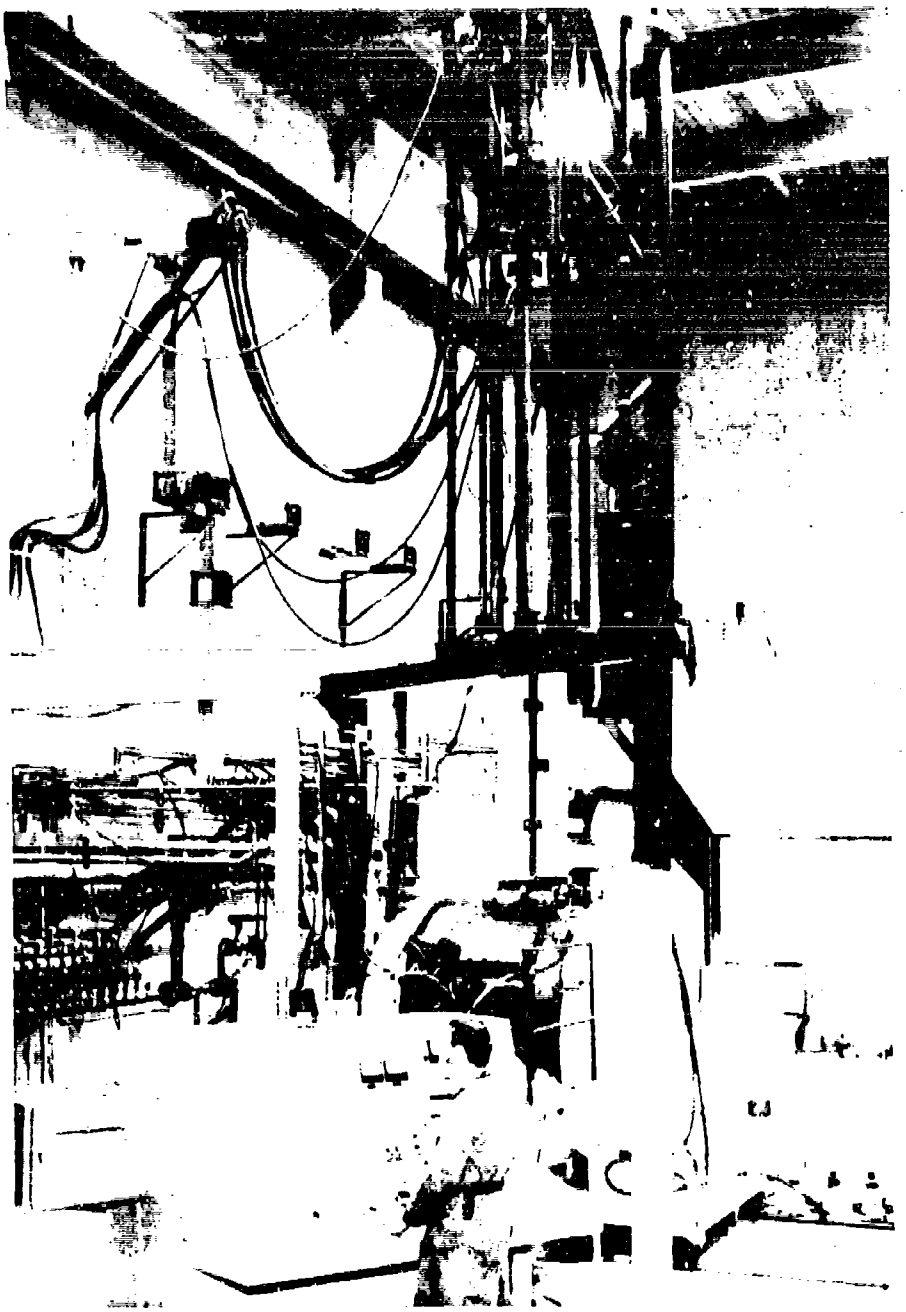

Figure 1. REM Consumable-Electrode Vacuum Casting Furnace.

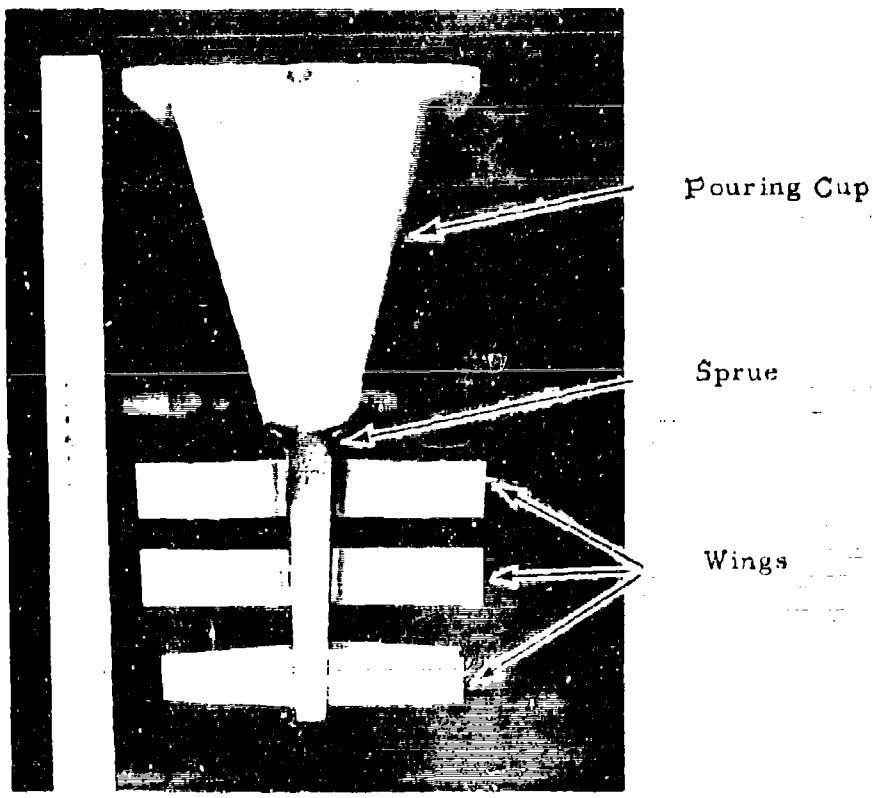

Figure 2. Wax Pattern of Fluidity Specimen.

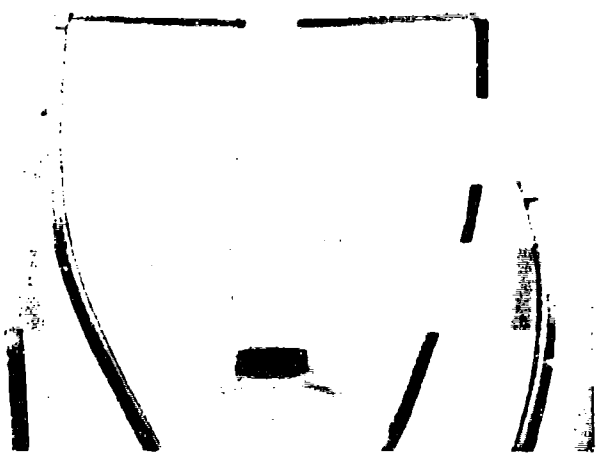

Figure 3. Wax Pattern of Vented Fluidity Specimen.

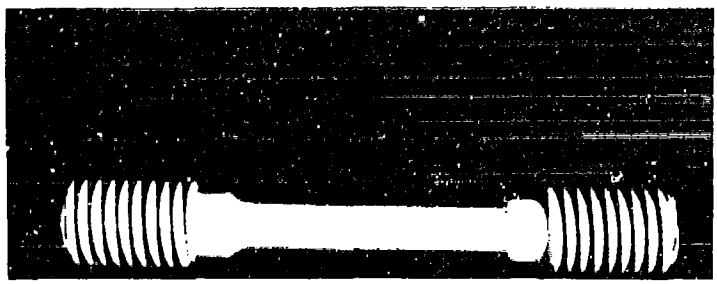

1 2 3 4

Tensile Specimen

1 2 3 4

Oxidation/Thermal Fatigue Test Paddle

Figure 4. Wax Patterns of Test Specimens.

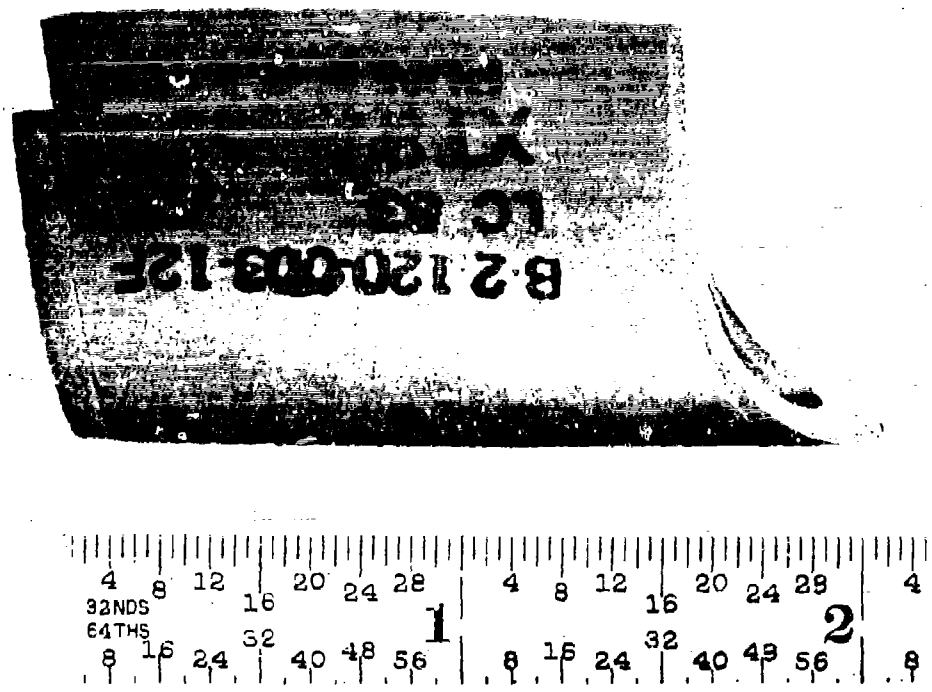

Figure 5. T55-L-11 First Stage Turbine Nozzle Vane.

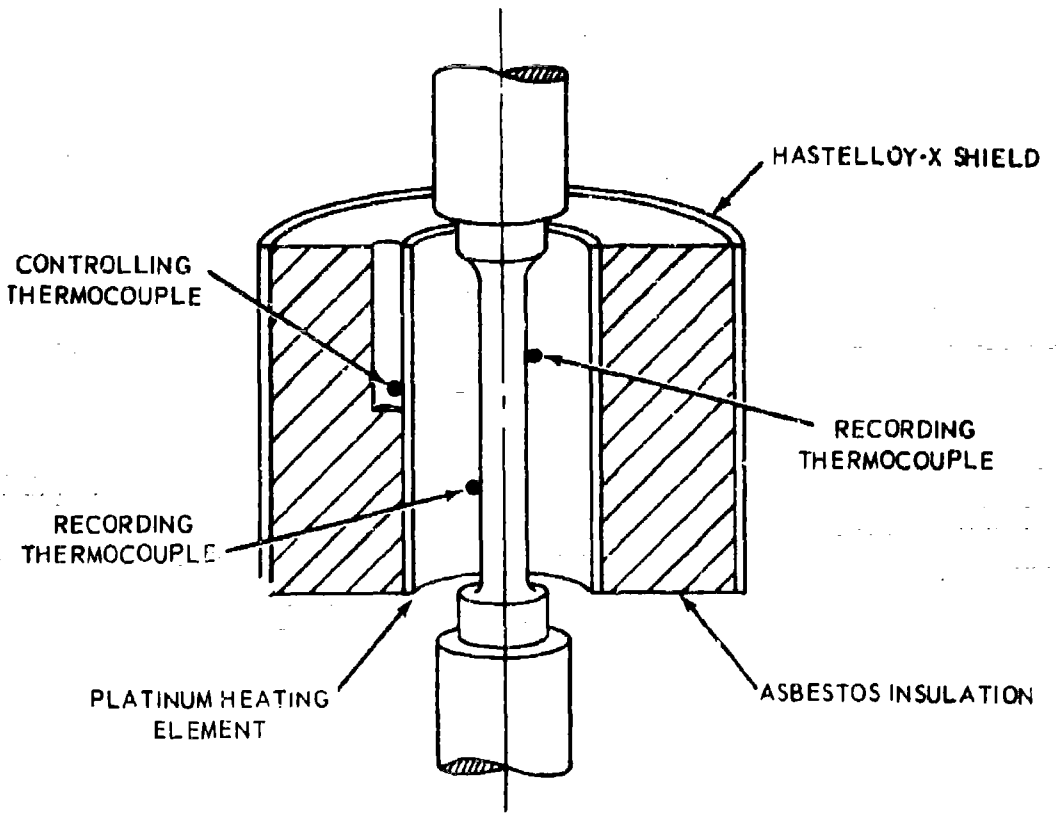

Figure 6. Stress-Rupture Heating Apparatus.

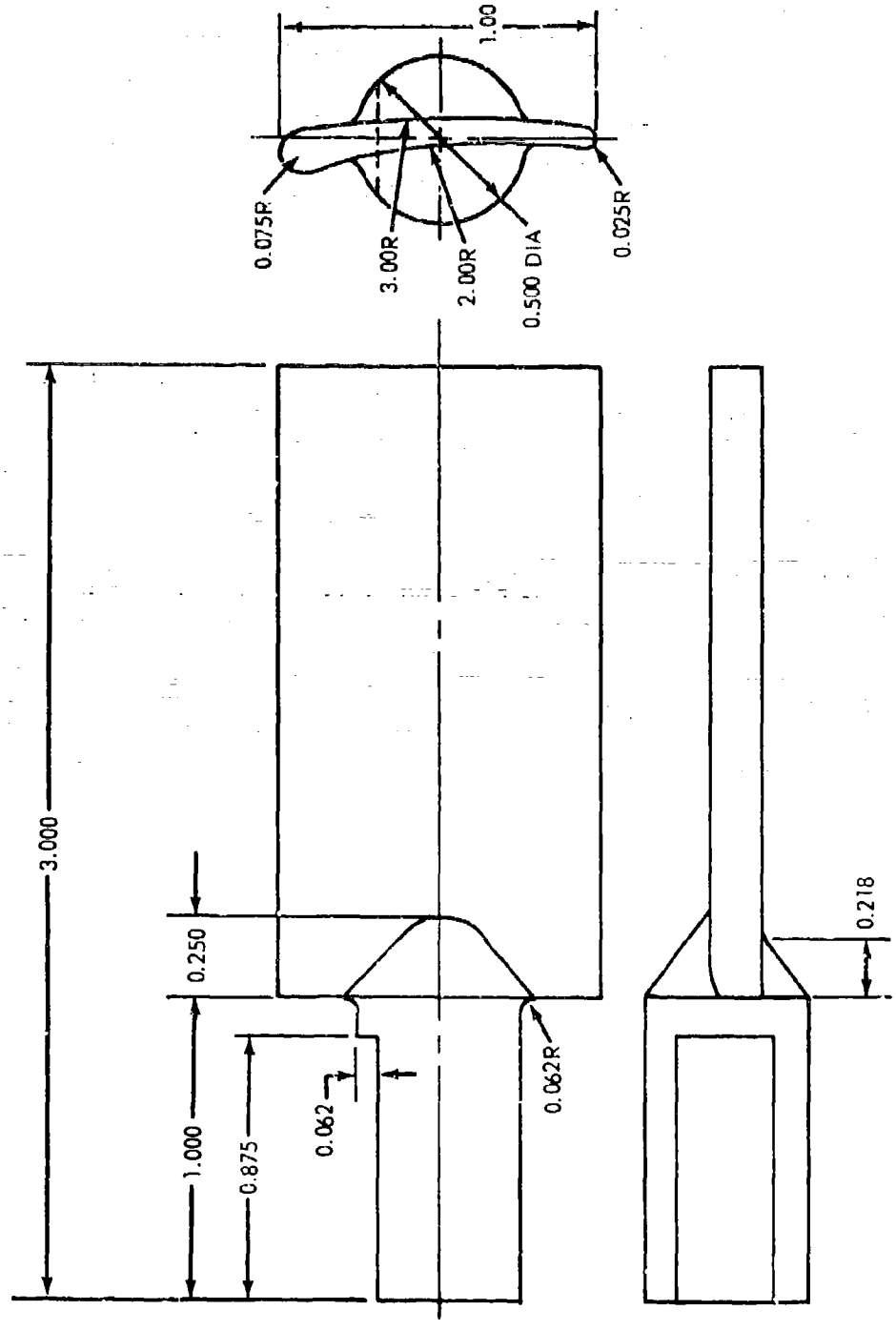

Figure 7. Dimensions of Oxidation Test Paddle.

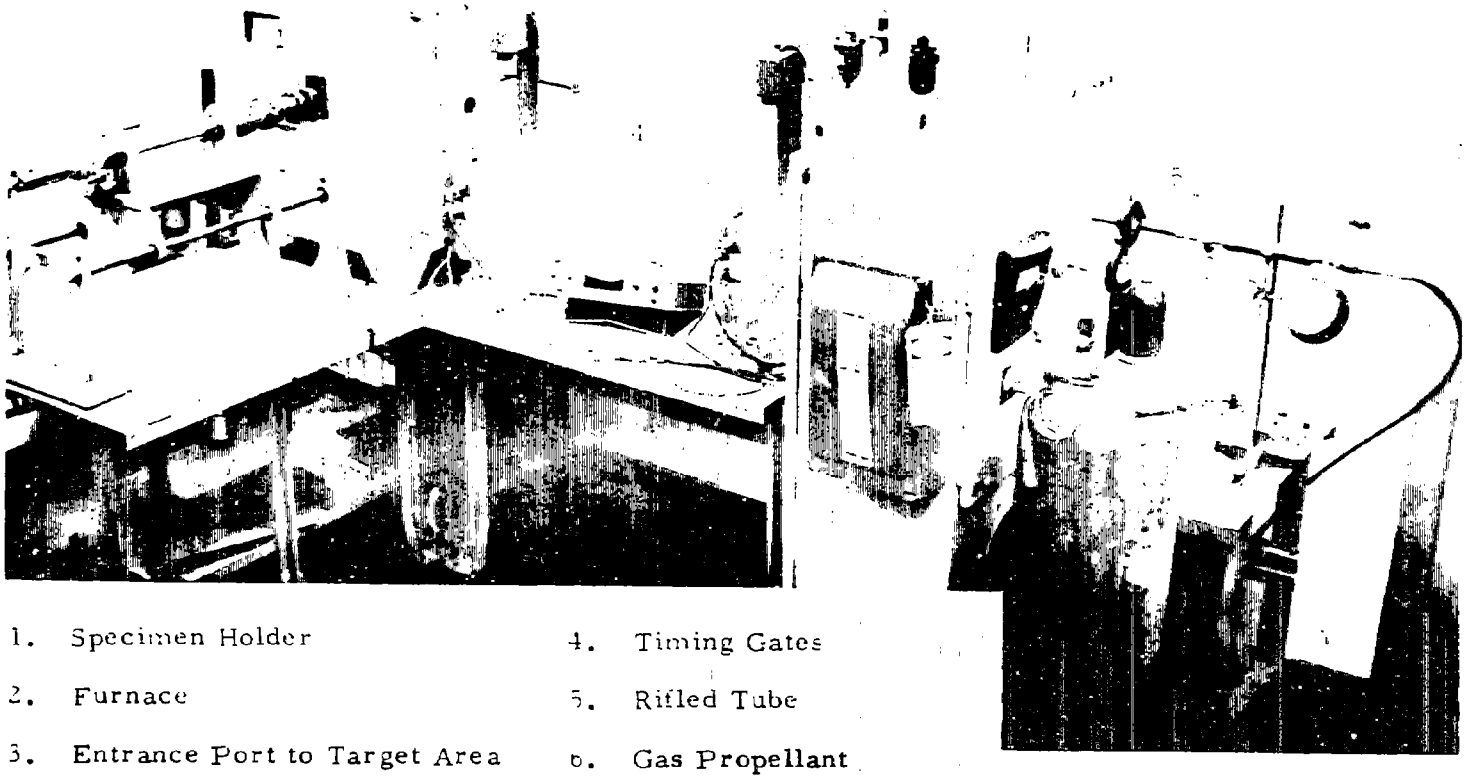

1. Specimen Holder
2. Furnace
3. Entrance Port to Target Area
4. Timing Gates
5. Rifled Tube
6. Gas Propellant

Figure 8. Avco Lycoming Ballistic - Impact Test Rig.

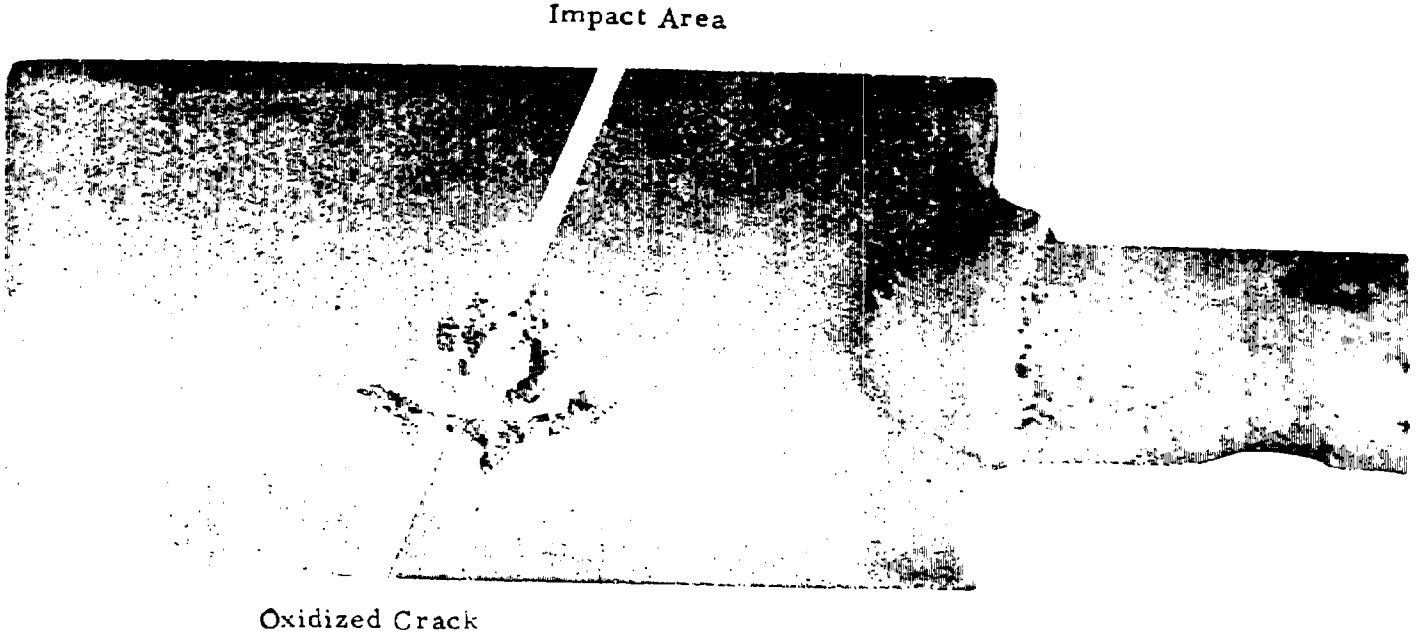

Figure 9. Coated B-66 Paddle Showing Ballistically Impacted Area.

Figure 10. Coated C-3015 Paddle Showing Ballistically Impacted Area.

Distressed Area

Figure 11. Coated C-3015 Paddle Showing Manually Distressed Area.

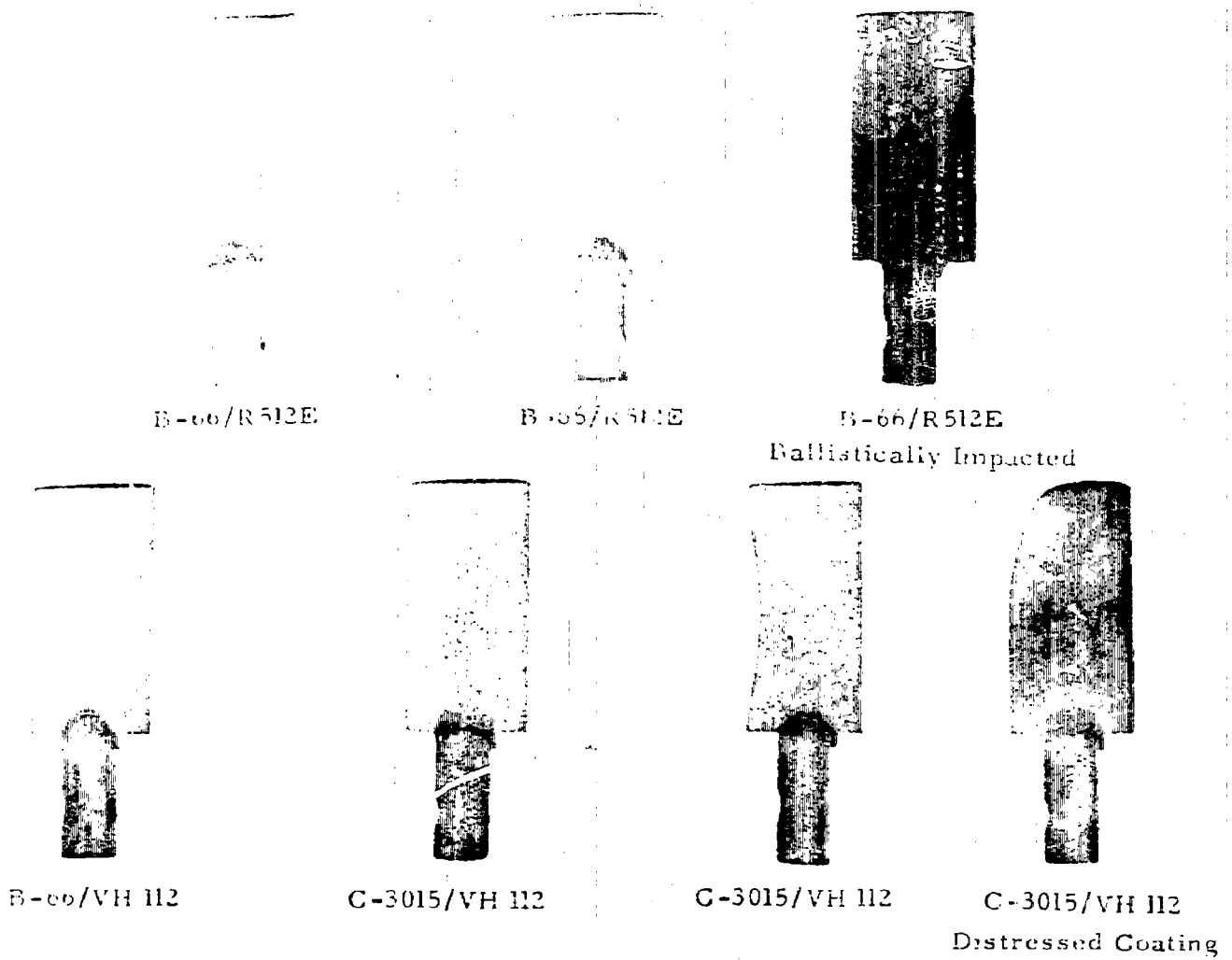

Figure 12. Coated B-66 and C-3015 Paddles Prior to Oxidation Testing.

(Arrows Indicate Non-Filled Areas Blended Prior to Coating).

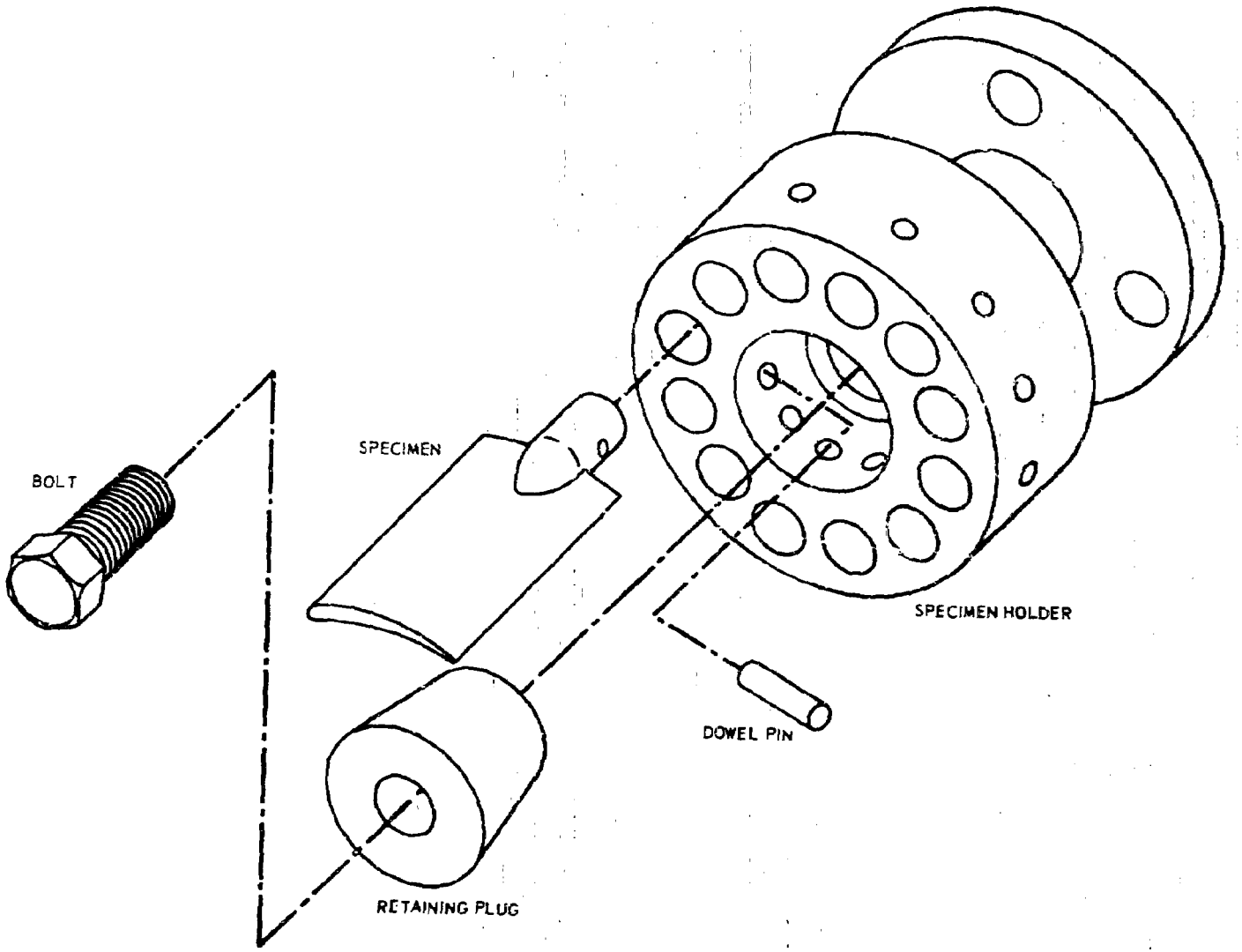

Figure 13. Attachment Scheme for Environmental Rig Testing.

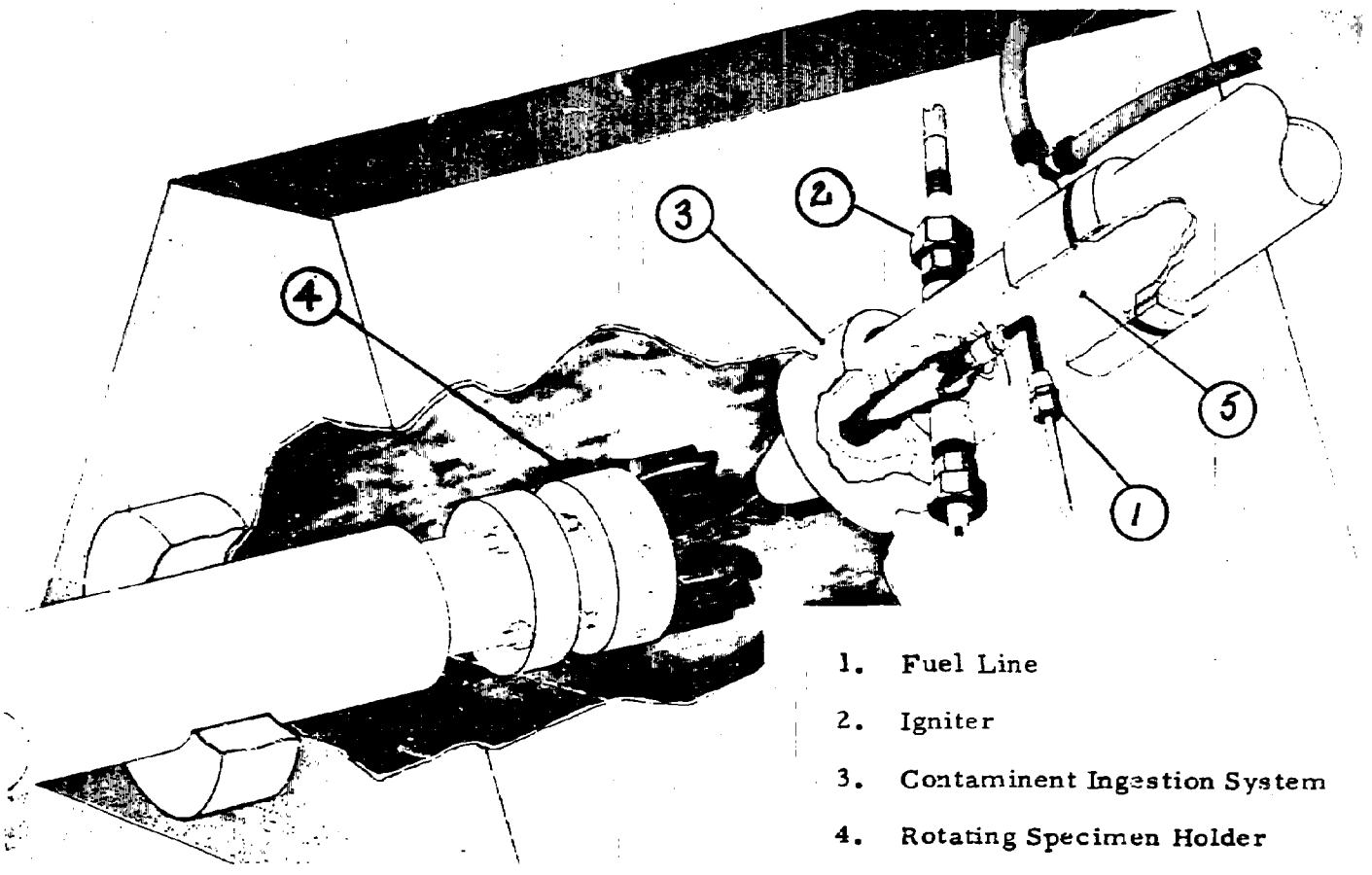

1. Fuel Line
2. Igniter
3. Contaminent Ingestion System
4. Rotating Specimen Holder
5. Preheated Air

Figure 14. Schematic of Environmental Rig Combustor.

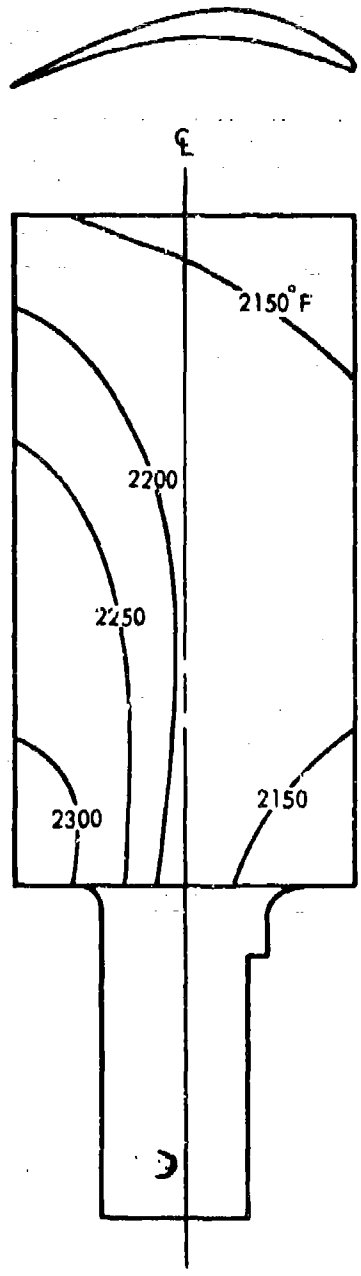

Figure 15. Temperature Distribution (°F) Obtained During Environmental Testing.

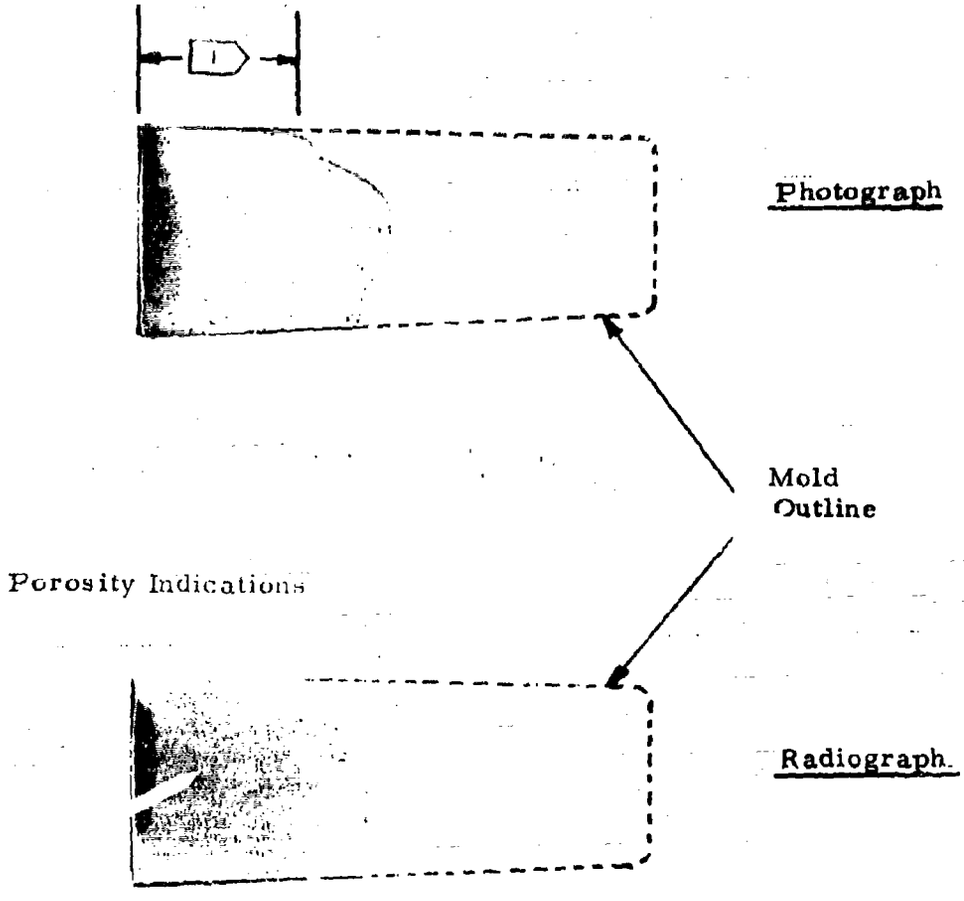

Figure 16. Method Used to Evaluate Fill and Porosity in Individual Fluidity Wing Castings.

Three Tungsten Layers
Unheated Mold

Two Tungsten Layers
Heated (1160°F) Mold

Figure 17. B-66 Fluidity Castings Showing Typical Fill.

Before

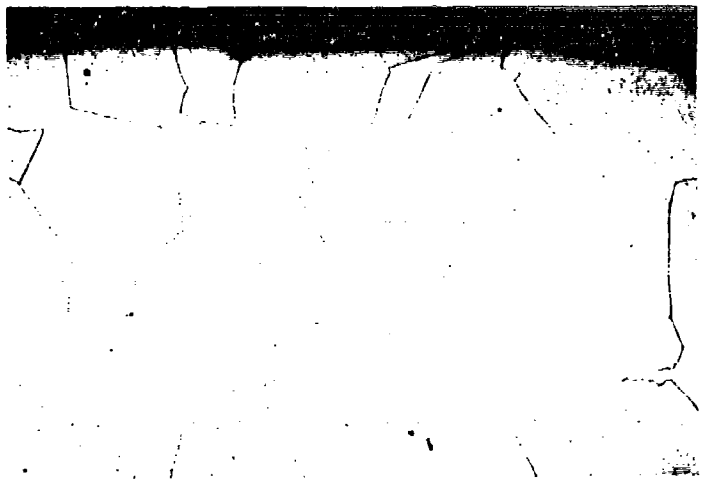

After

Etchant: 5 HNO_3, 14 H_2 SO_4, 20 HF, 50 H_2O Mag.: 100X

Figure 18. As-Cast Appearance of B-66 Surfaces Before and After Etch Technique Modification.

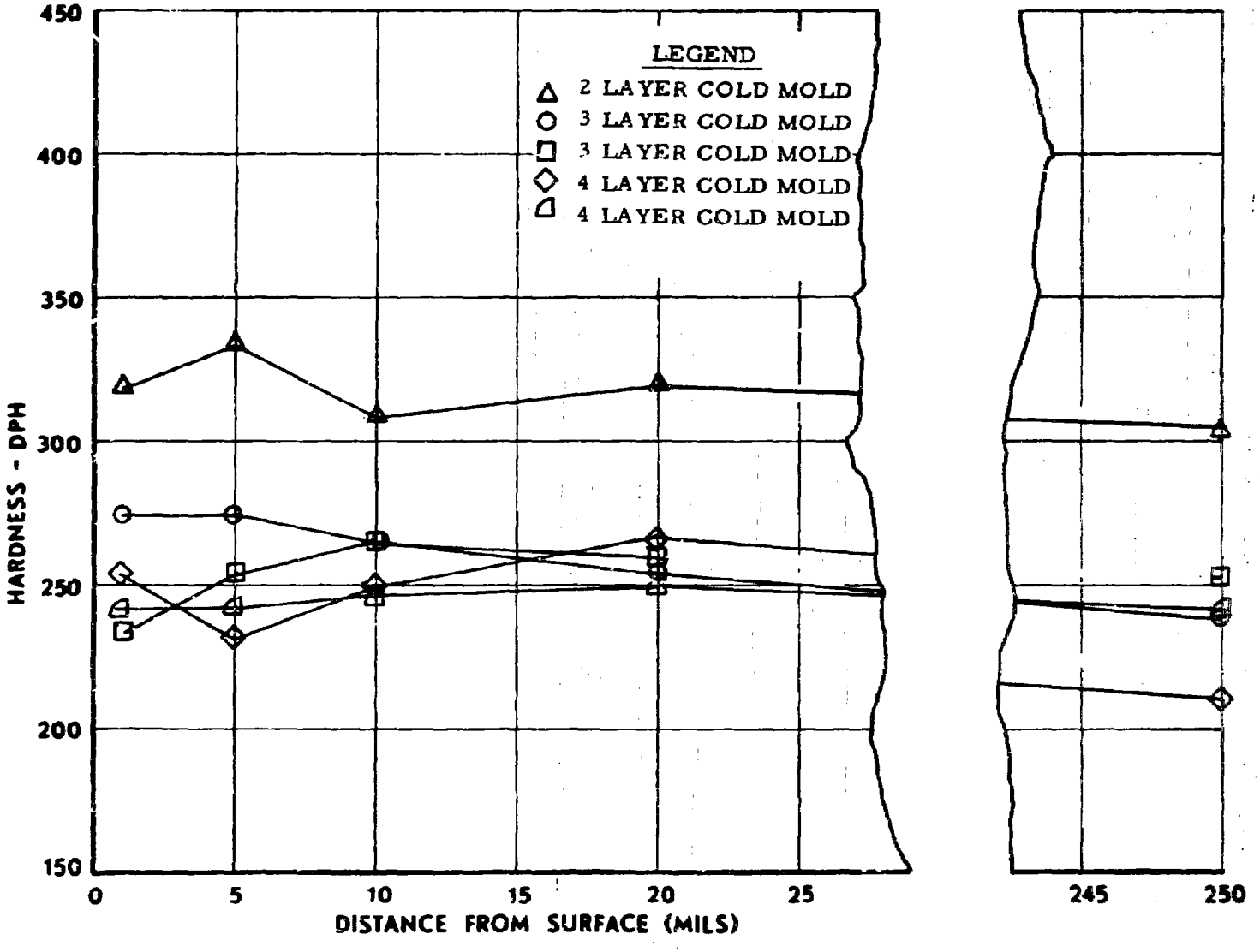

Figure 19. Microhardness Surveys of B-66 Fluidity Castings.

Three Tungsten Layers
Unheated Mold

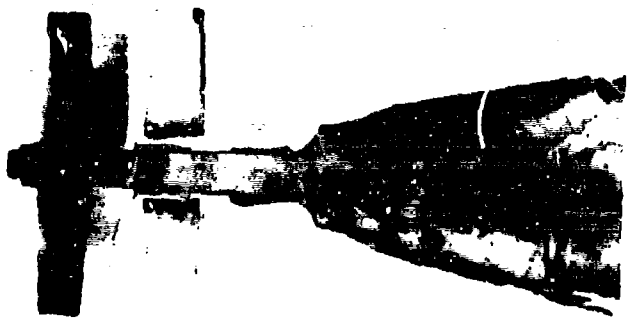

Two Tungsten Layers
Heated (1400°F) Mold

Figure 20. C-3015 Fluidity Castings Showing Typical Fill.

Mag.: 100X

Mag.: 500X

Etchant: Anodized

Figure 21. Typical Surface Microstructure of C-3015 Alloy Cast Into Fluidity Molds.

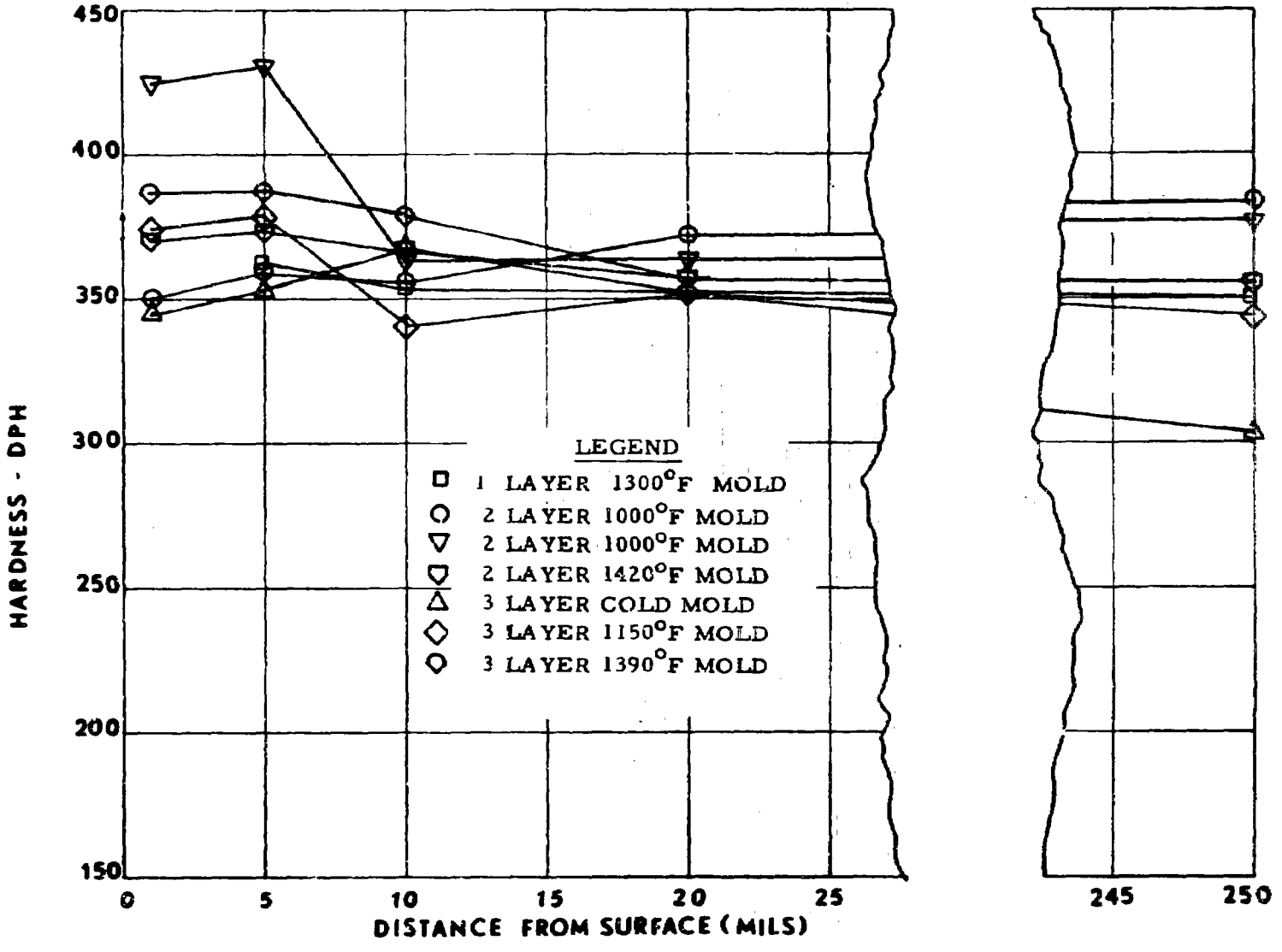

Figure 22. Microhardness Surveys of C-3015 Fluidity Castings.

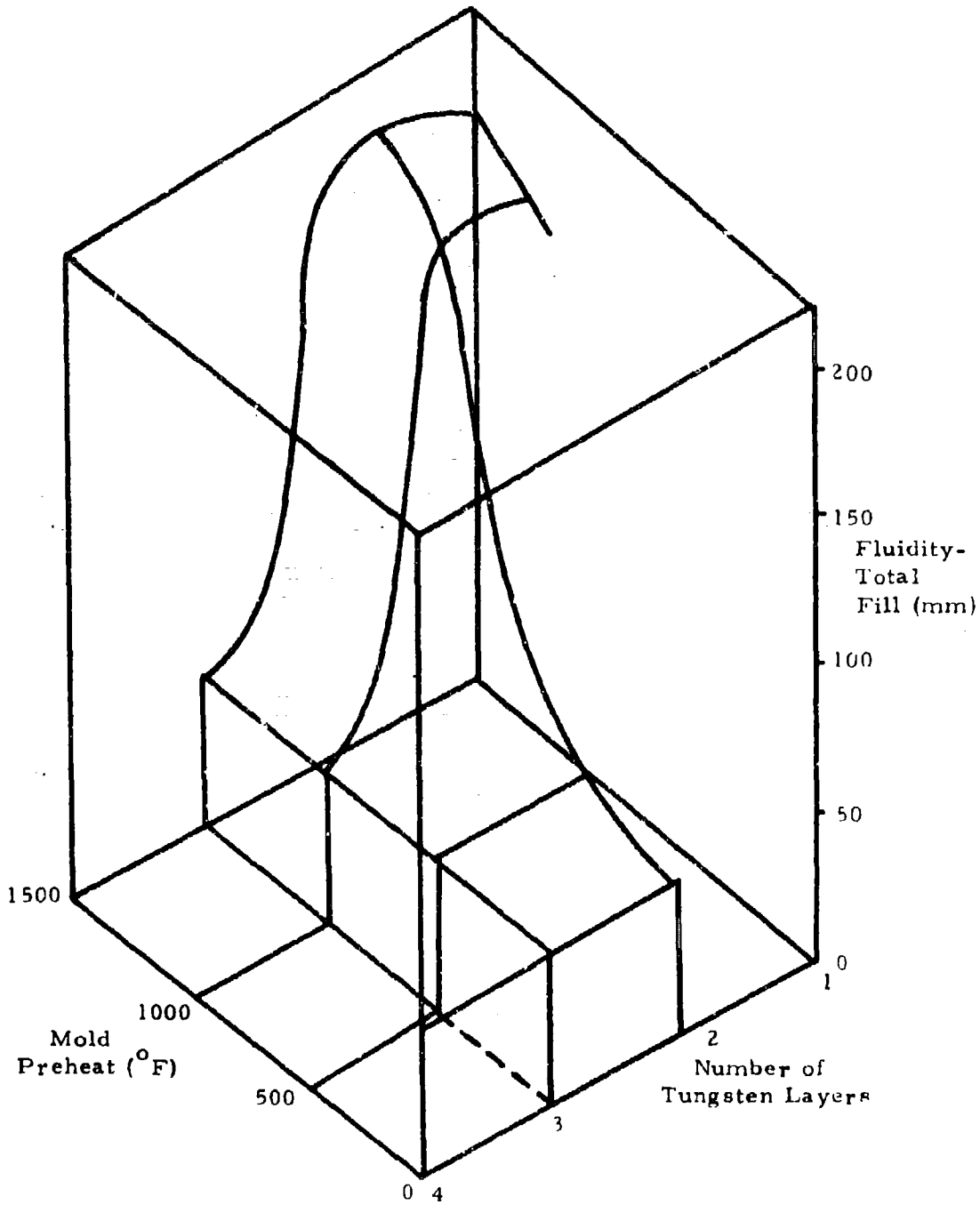

Figure 23. Effect of Mold Preheat and Tungsten Coating Thickness on Fluidity of Cast Columbium Alloys.

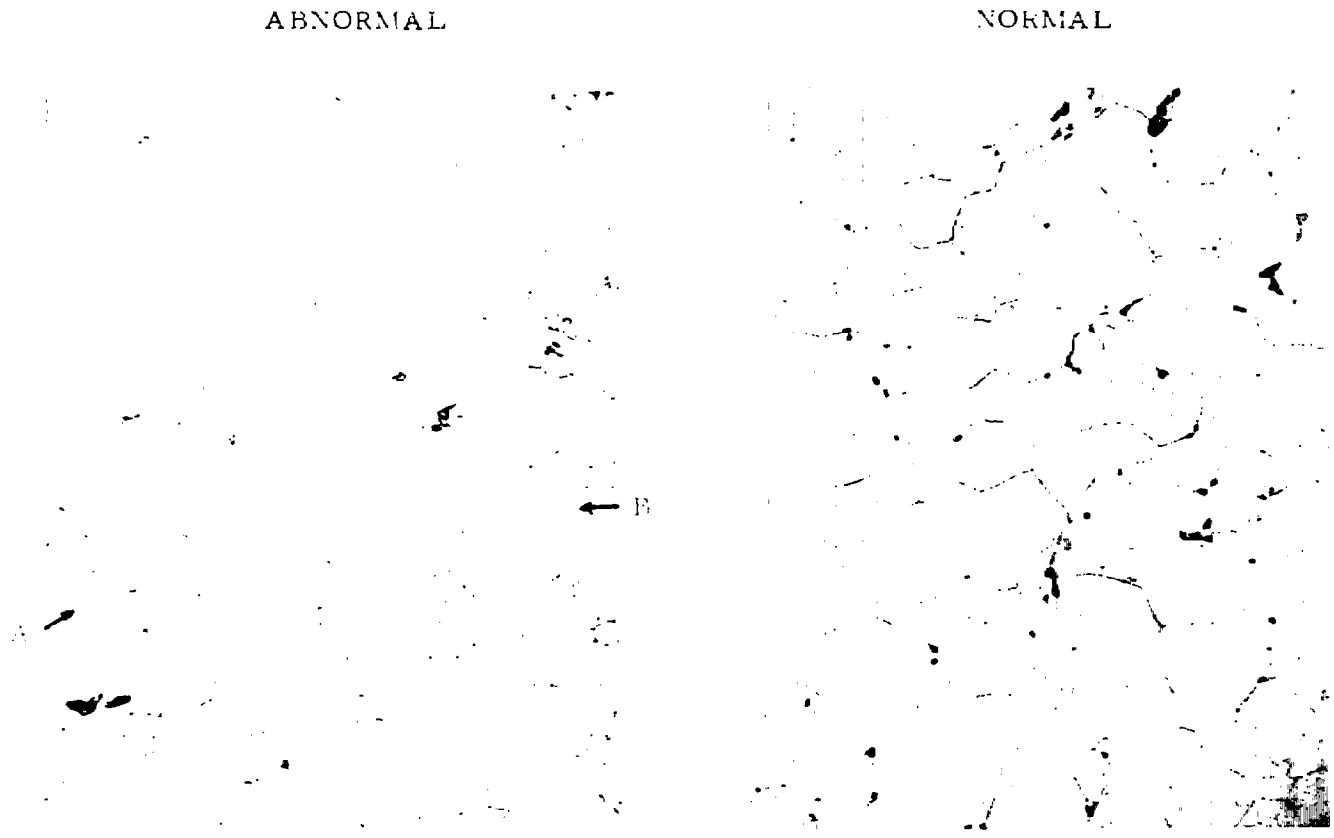

Figure 24. Abnormal and Normal Microstructure of B-66 Alloy. Arrow A Points to Matrix Area, While Arrow B Indicates Area of Suspected Contamination.

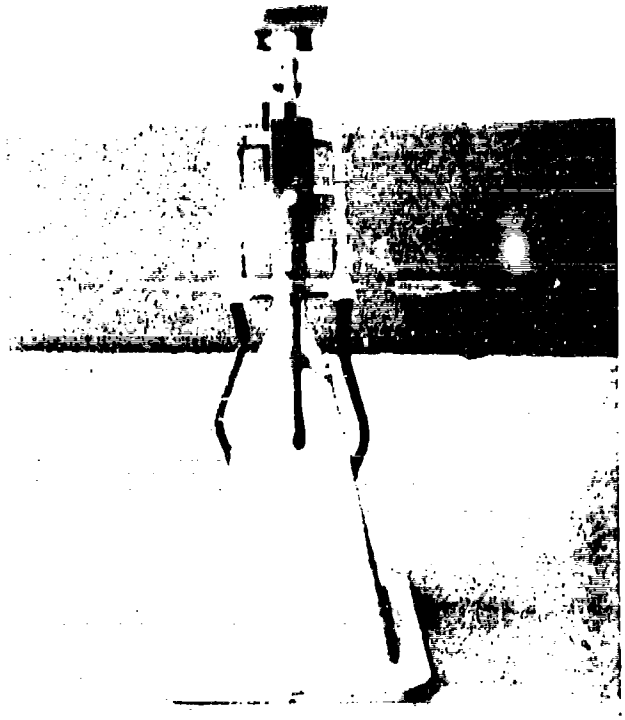

Figure 25. Wax Pattern Depicting Gating Techniques.

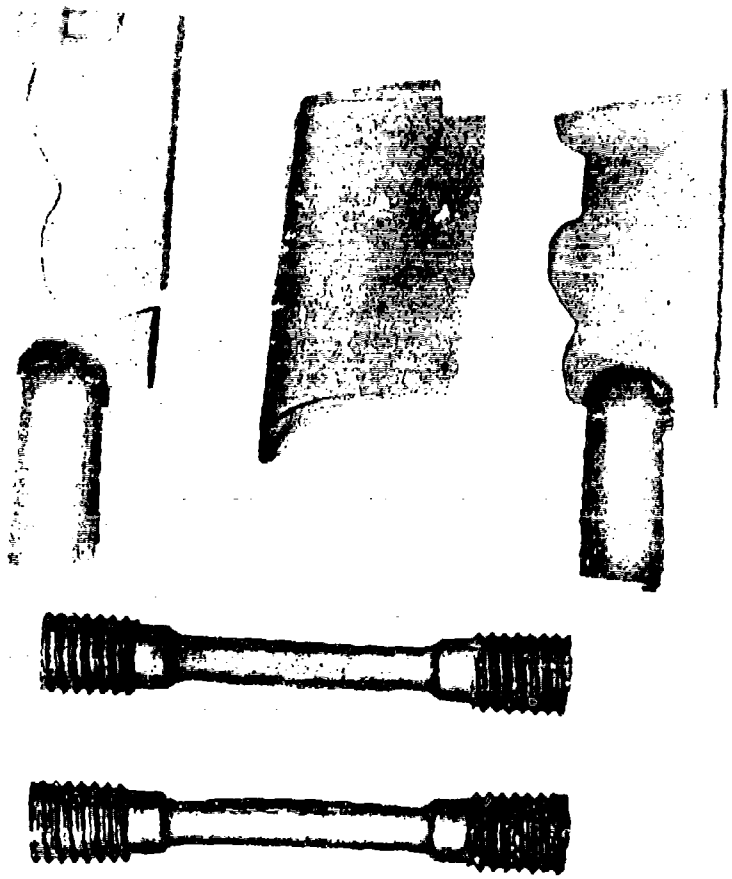

Figure 26. Specimens Cast in C-3015 Alloy During Gating Evaluation.

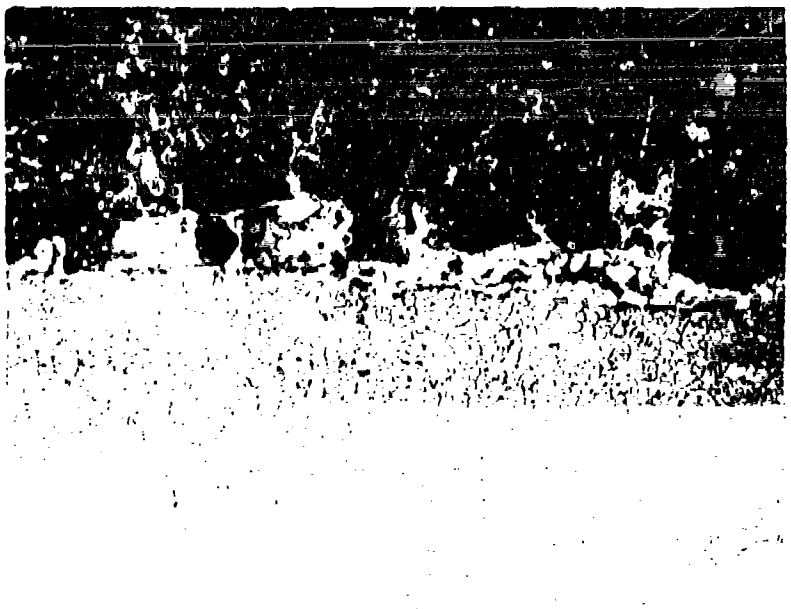

Etchant: Anodized Mag.: 128X

Figure 27. Abnormal Microstructure of C-3015 Alloy.

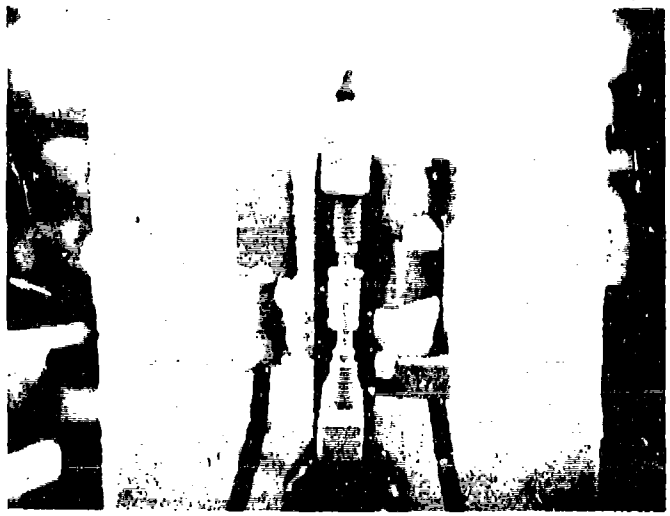

Configuration A

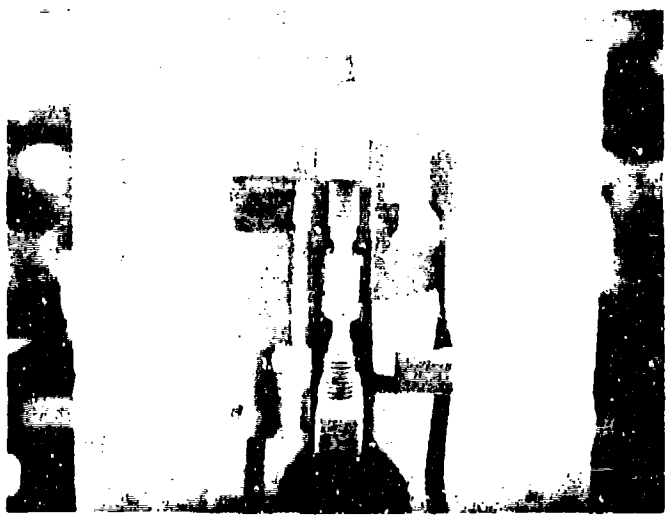

Configuration B

Figure 28. Modified Gating Arrangements of Two Wax Patterns.

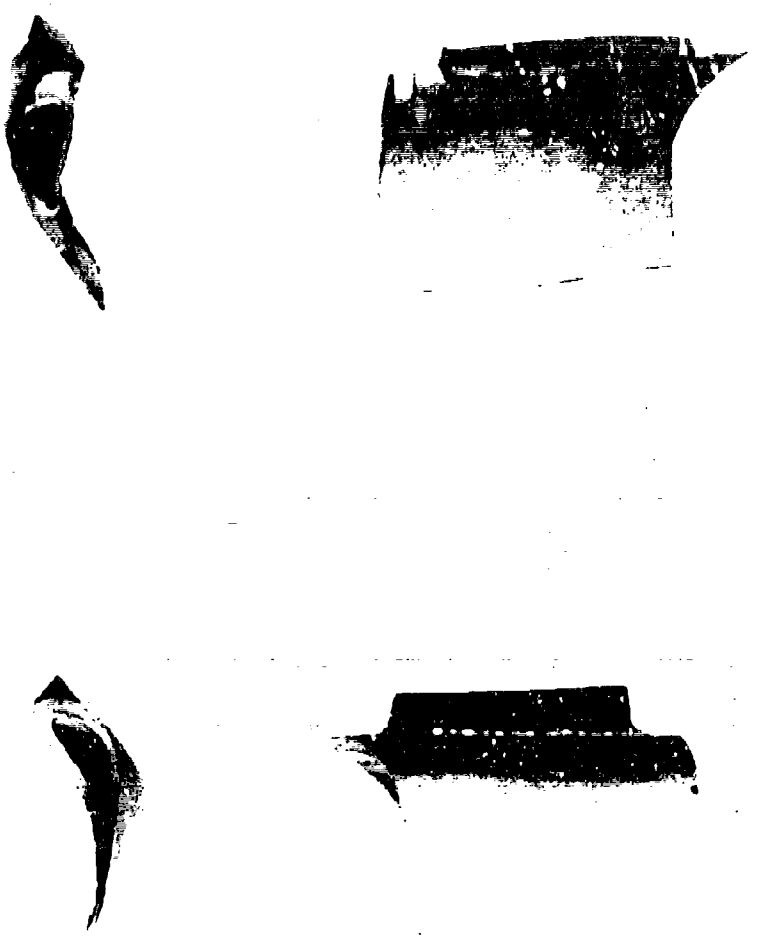

Figure 29. B-66 Hollow-Core Vane Showing Good Fill.

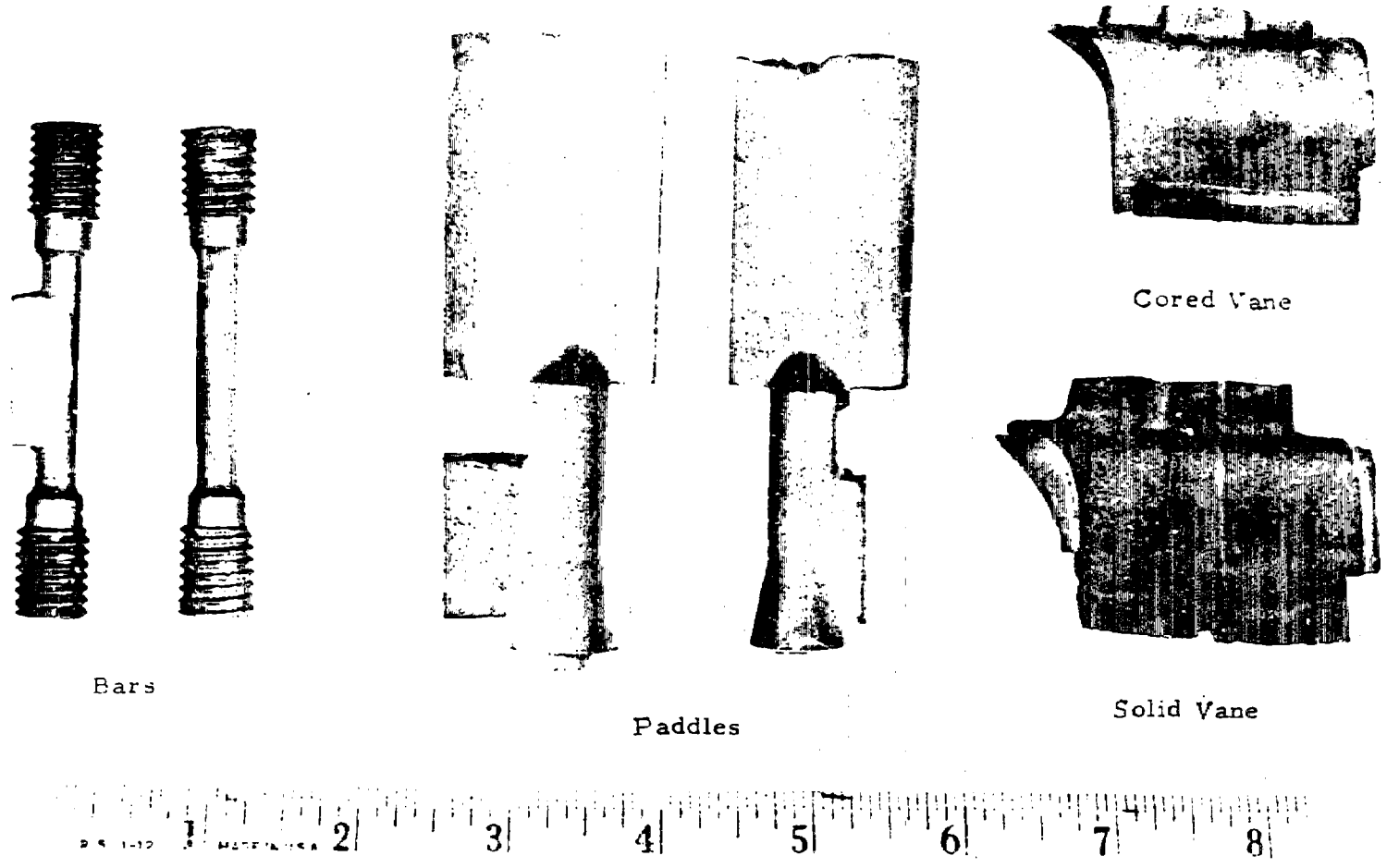

Figure 30. Typical Columbium Alloy Castings.

Figure 31. Electron Photomicrograph of Cast B-6 Alloy.

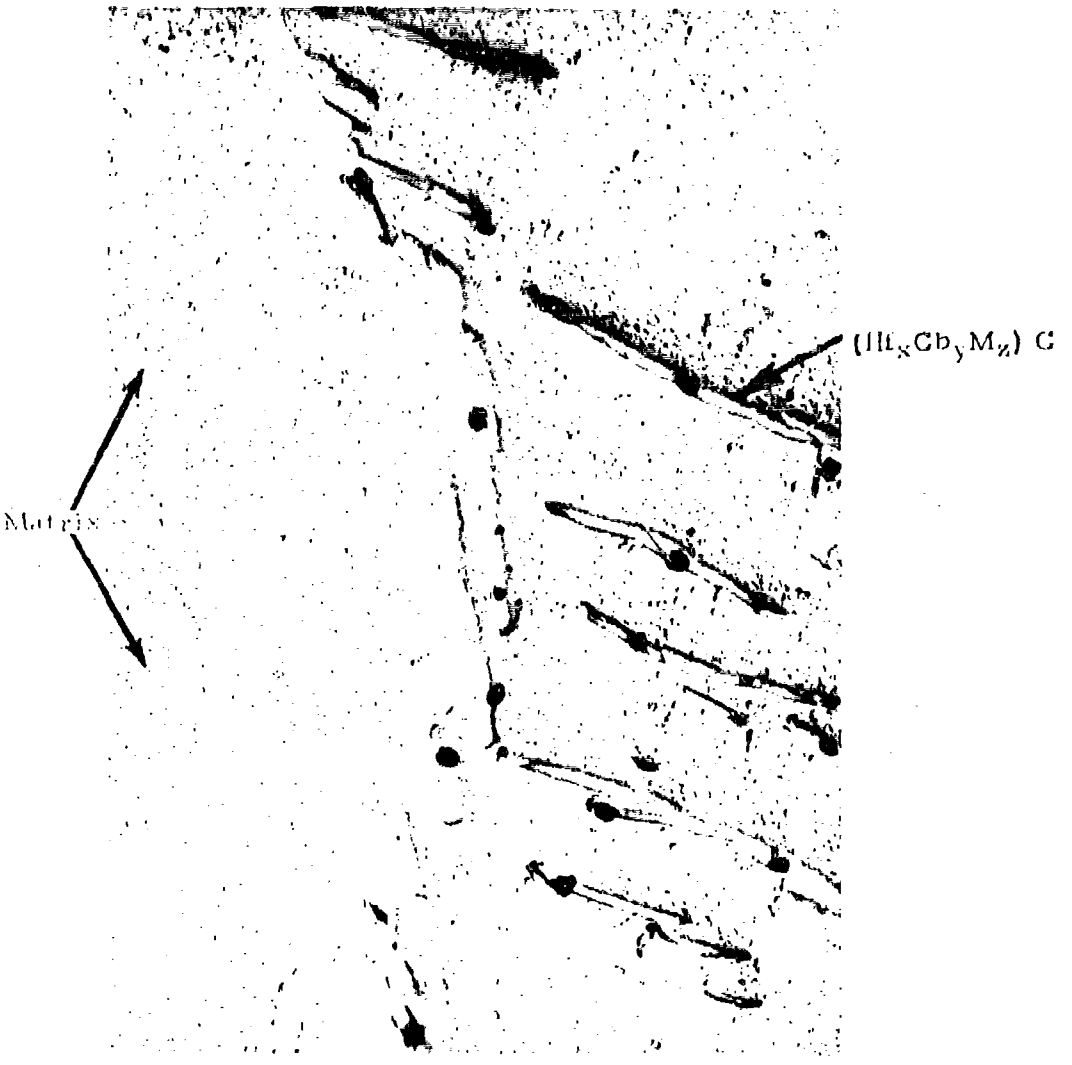

Figure 32. Electron Photomicrograph of Cast C-3015 Alloy.

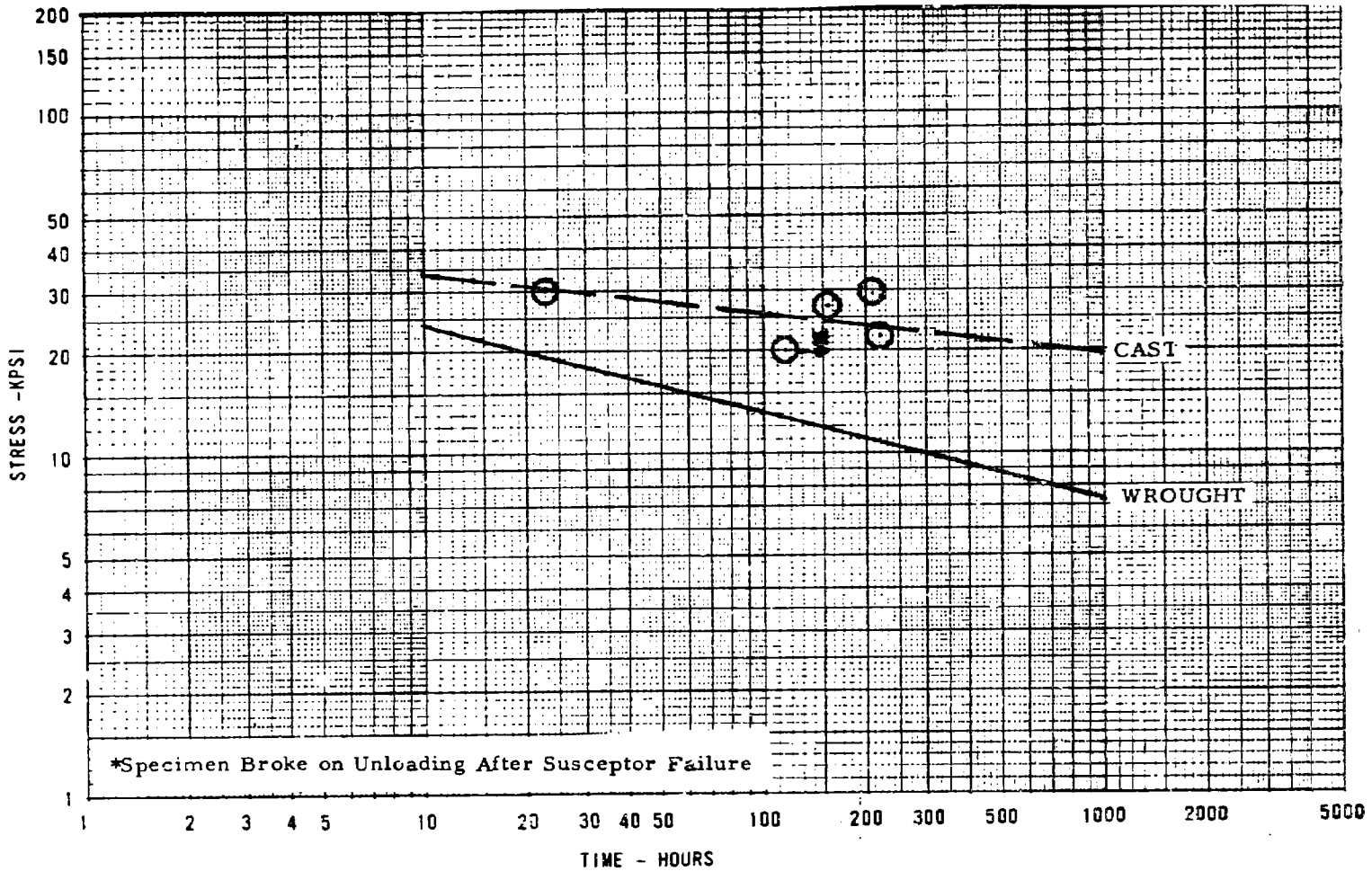

Figure 33. Stress-Rupture Testing of Cast and Wrought C-3015 Alloys at 2200°F.

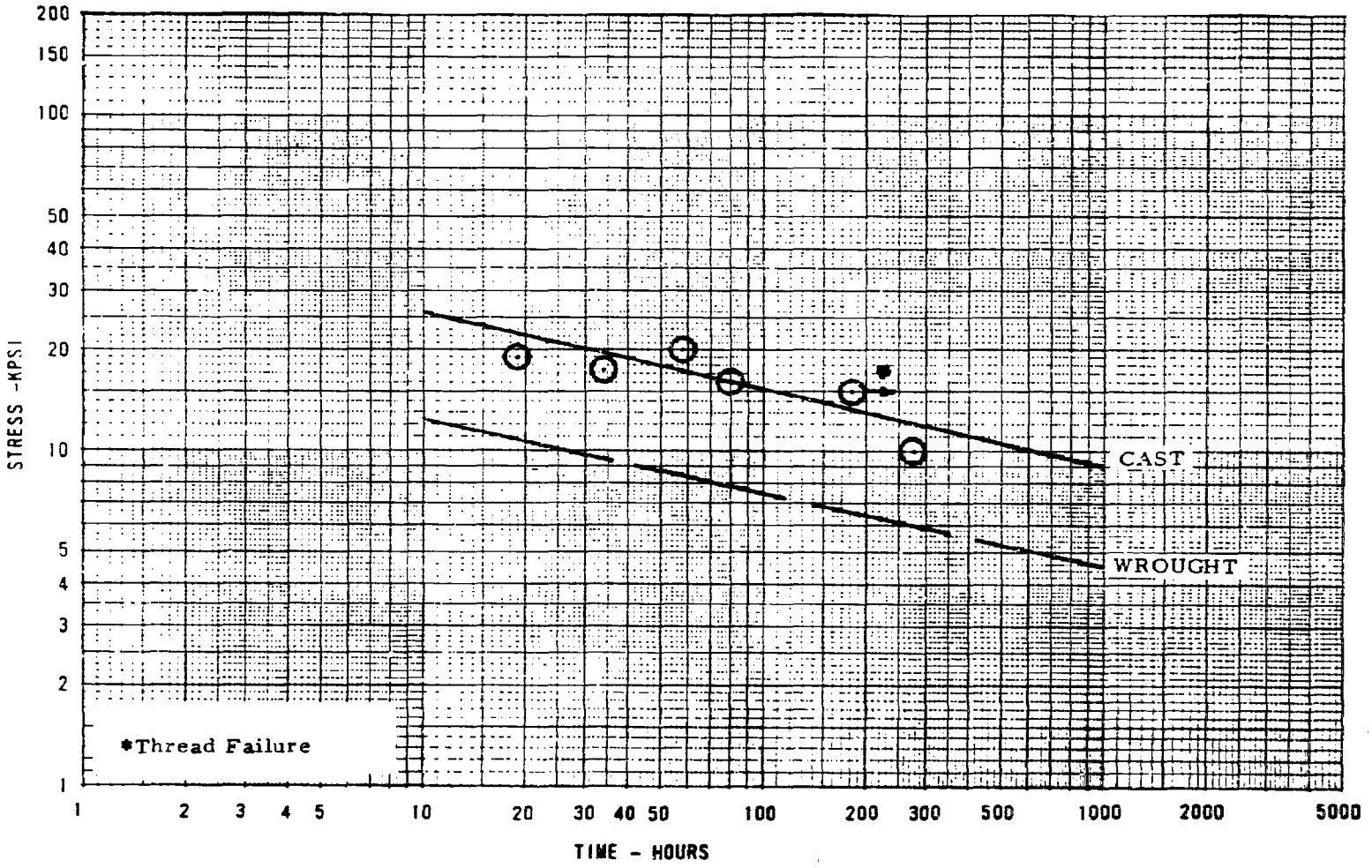

Figure 34. Stress-Rupture Testing of Cast and Wrought B-66 Alloys at 2200°F.

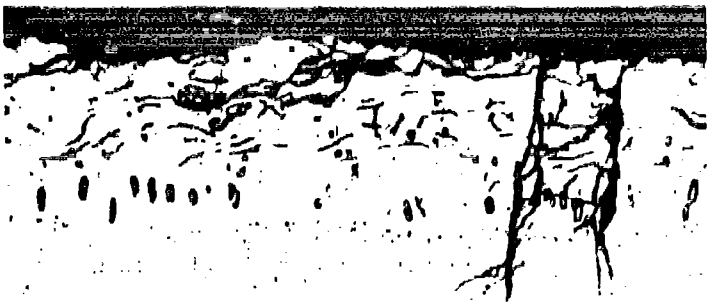

R512E Coated B-66

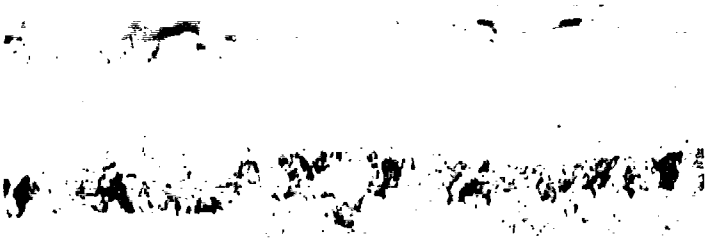

VH112 Coated C-3015

Etchant: 5 HNO_3, 14 H_2SO_4, 20 HF, 50 H_2O Mag.: 300X

Figure 35. Coating Cracks in Untested Specimens of Columbium Alloy.

Unetched Mag.: 300X

Figure 36. Tip Radius Cracking on Untested R512E Coated B-66.

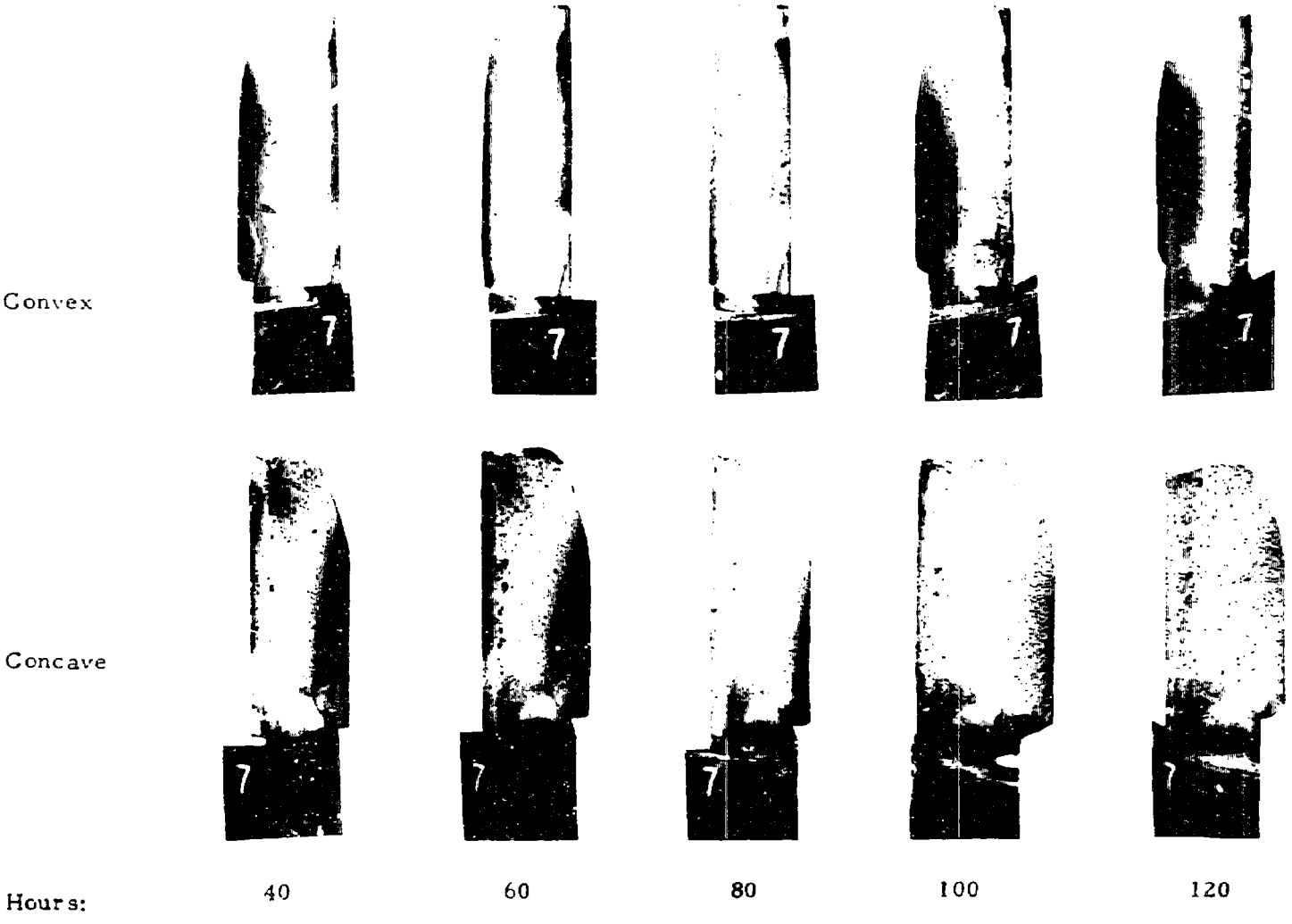

Figure 37. Condition of C-3015 Paddle During 120-Hour Test Showing Degradation of VH 112 Coating (See Arrow).

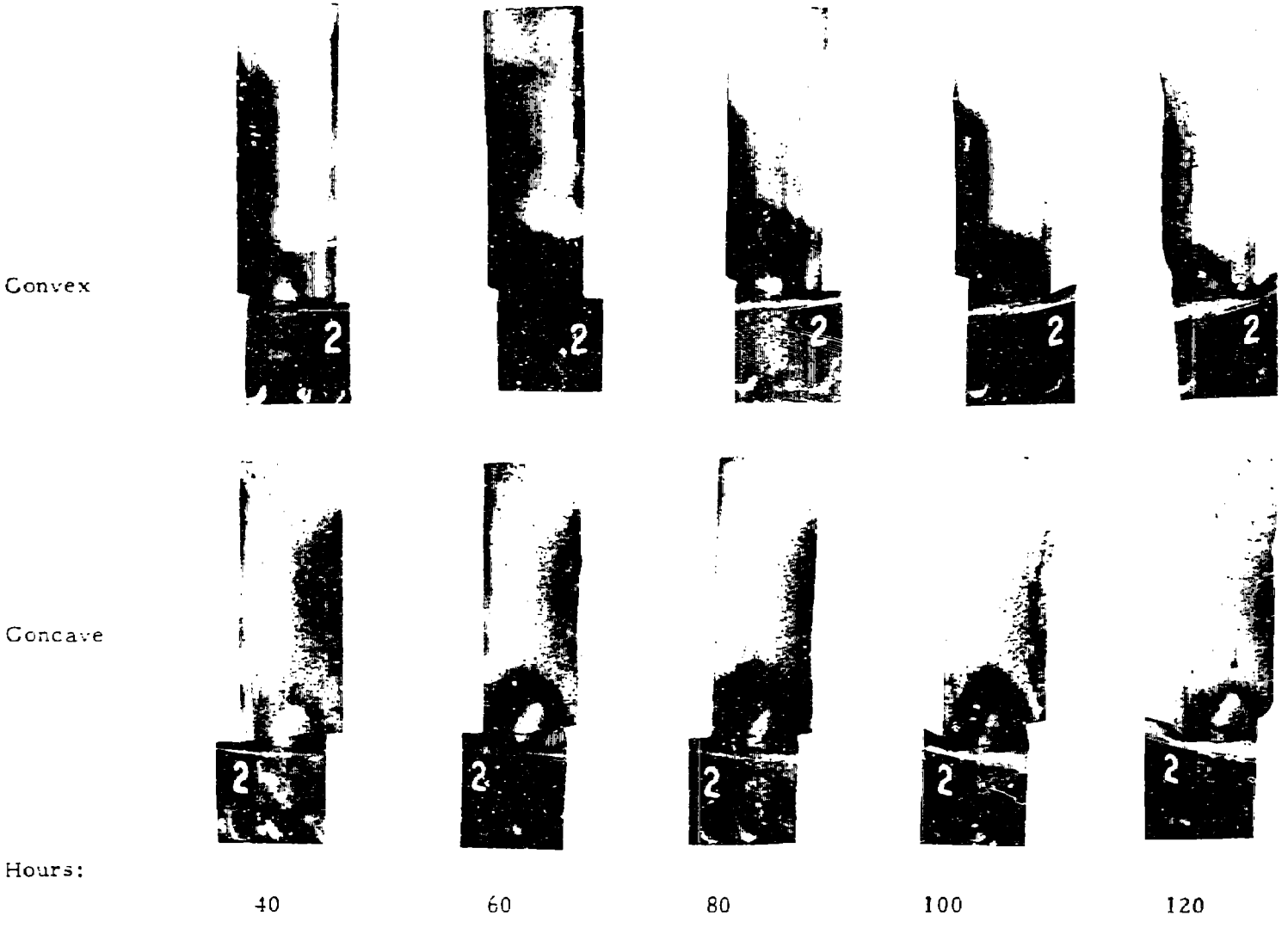

Figure 38. Condition of B-66 Paddle During 120-Hour Test Showing Degradation of VH 112 Coating.

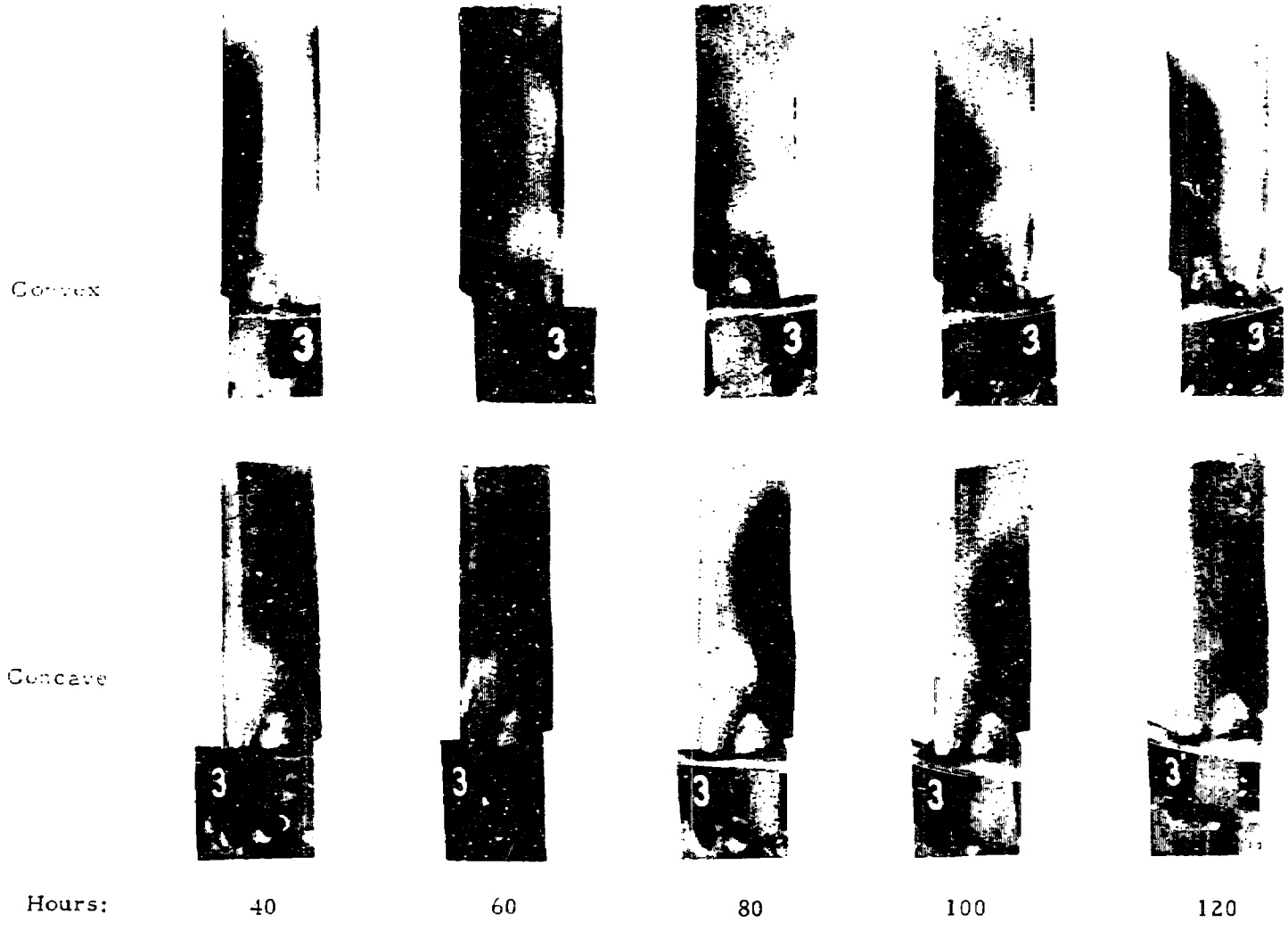

Figure 39. Condition of B-66 Paddle During 120-Hour Test Showing Degradation of R512E Coating.

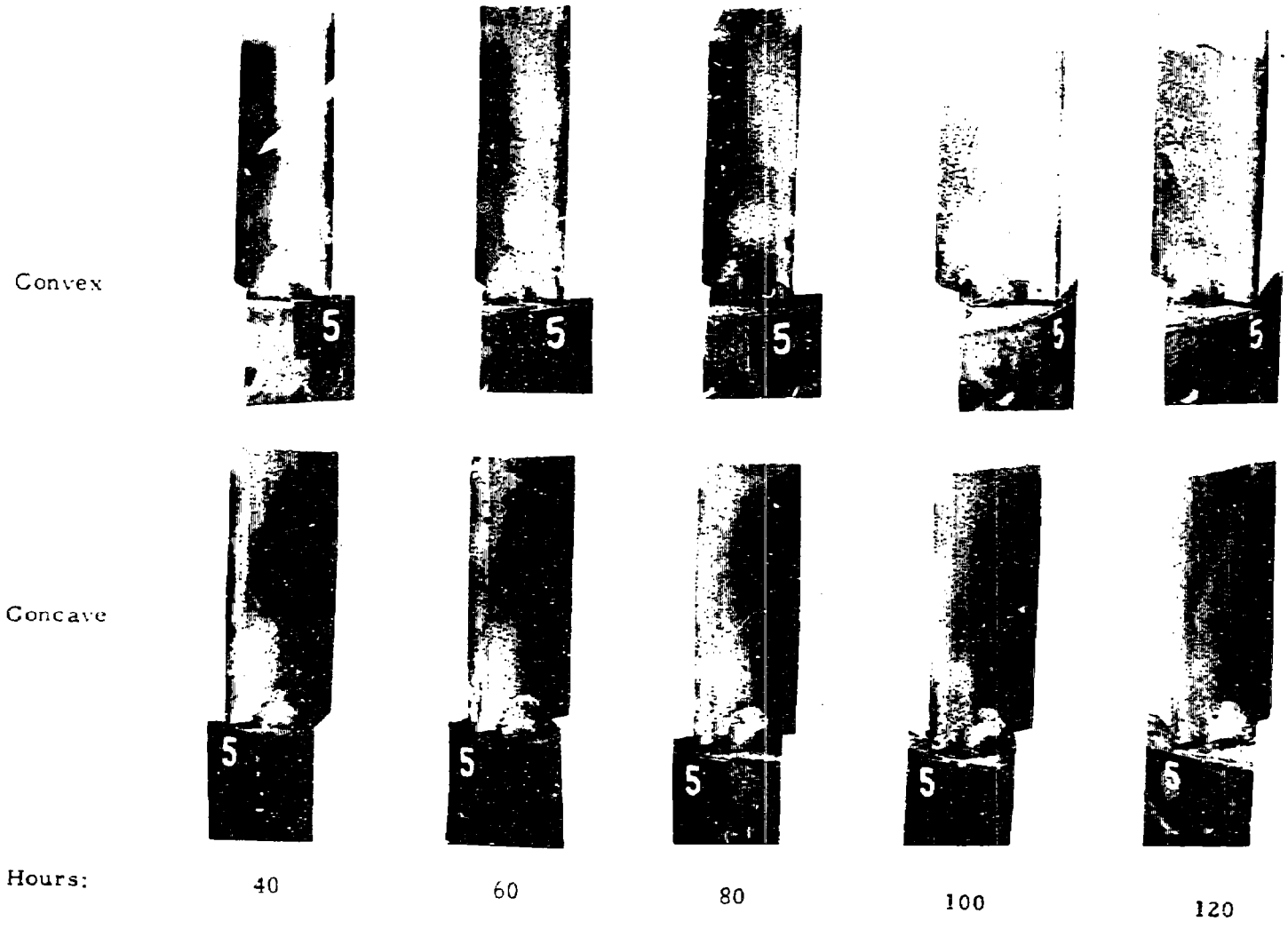

Figure 40. Condition of B-66 Paddle During 120-Hour Test (See arrow) Showing Degradation of Ballistically Impacted R512E Coating.

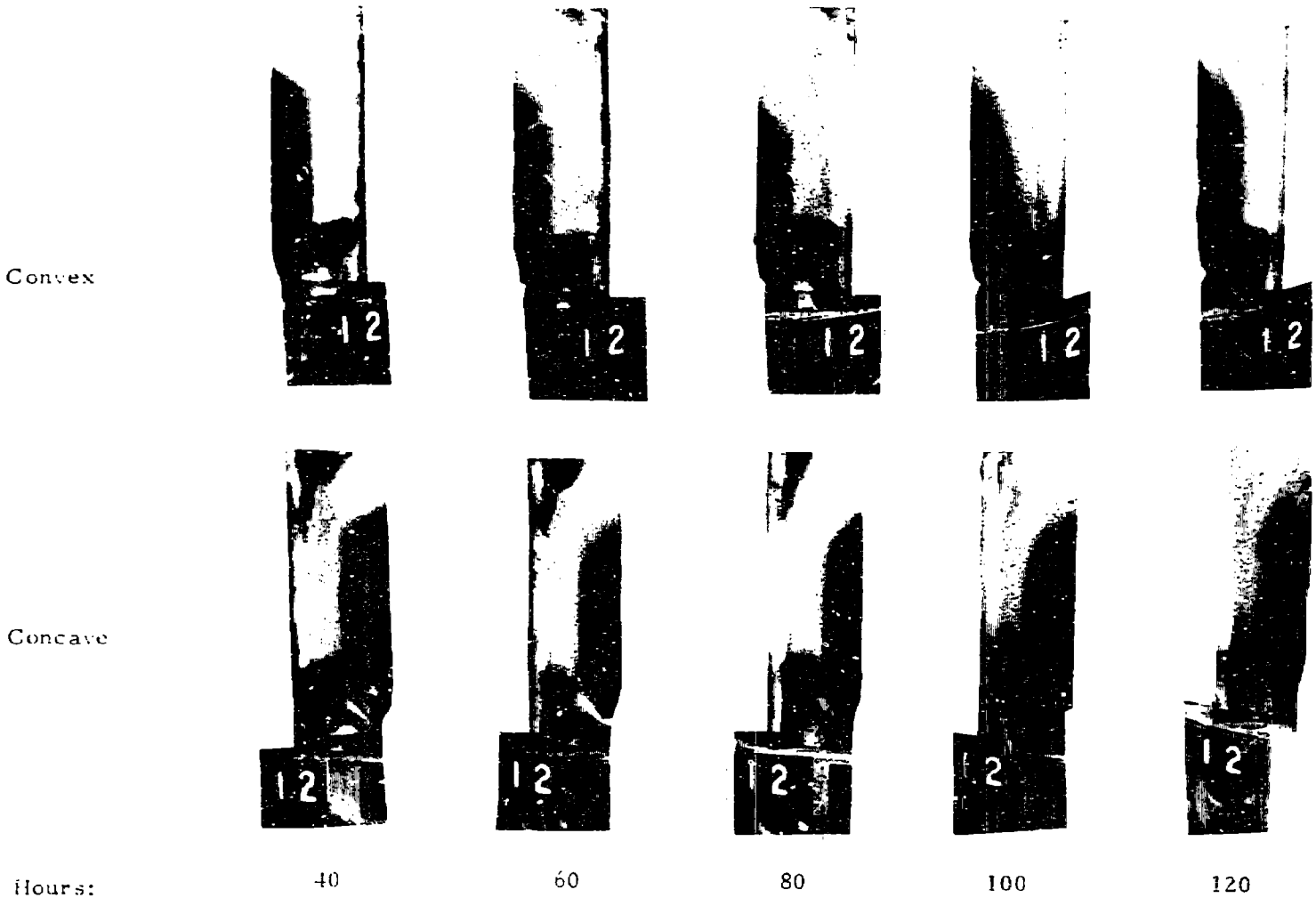

Figure 41. Condition of M3608 Paddle During 120-Hour Test Showing Degradation of 701 Coating.

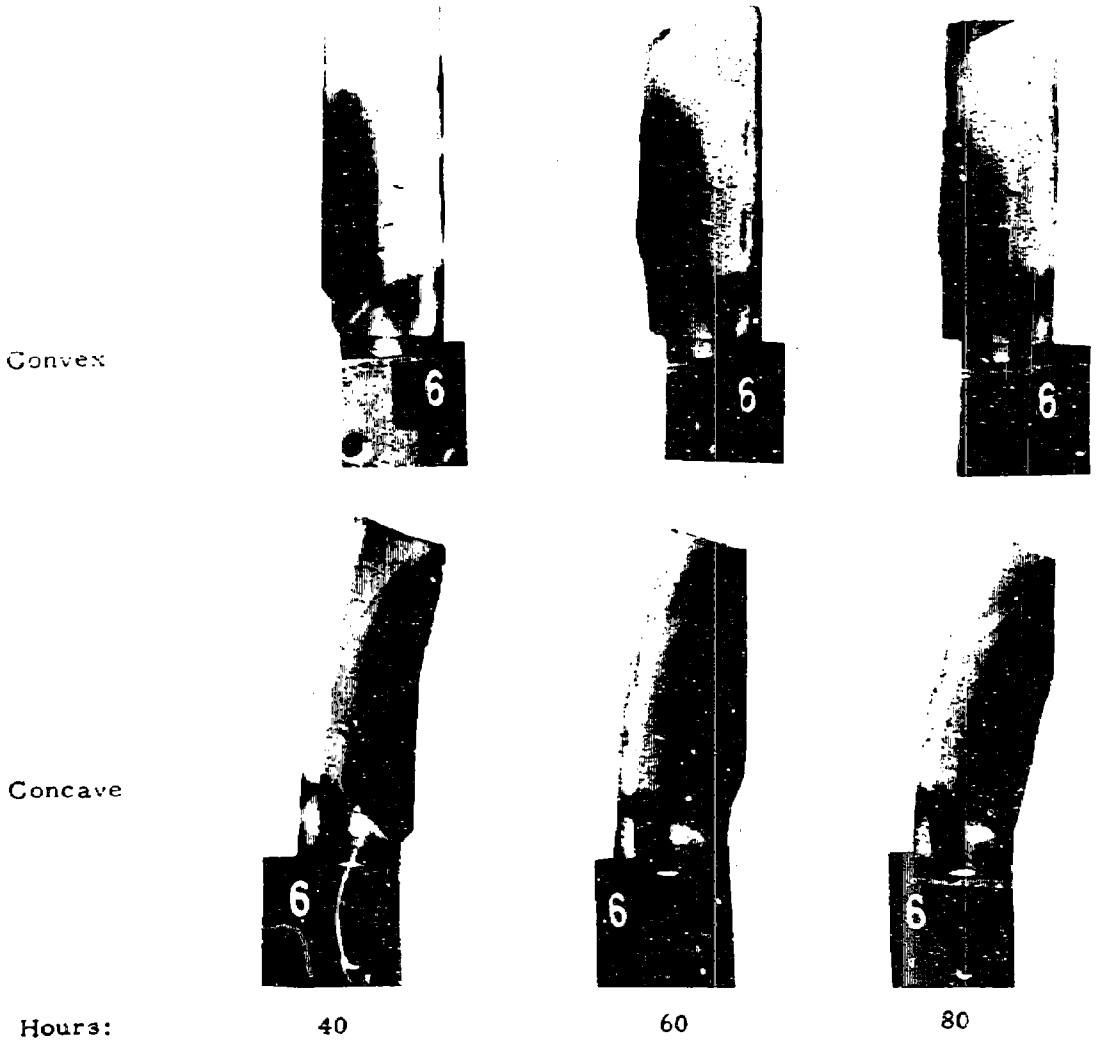

Figure 42. Condition of Inco 713C Paddle During 80-Hour Test Showing Degradation of 701 Coating.

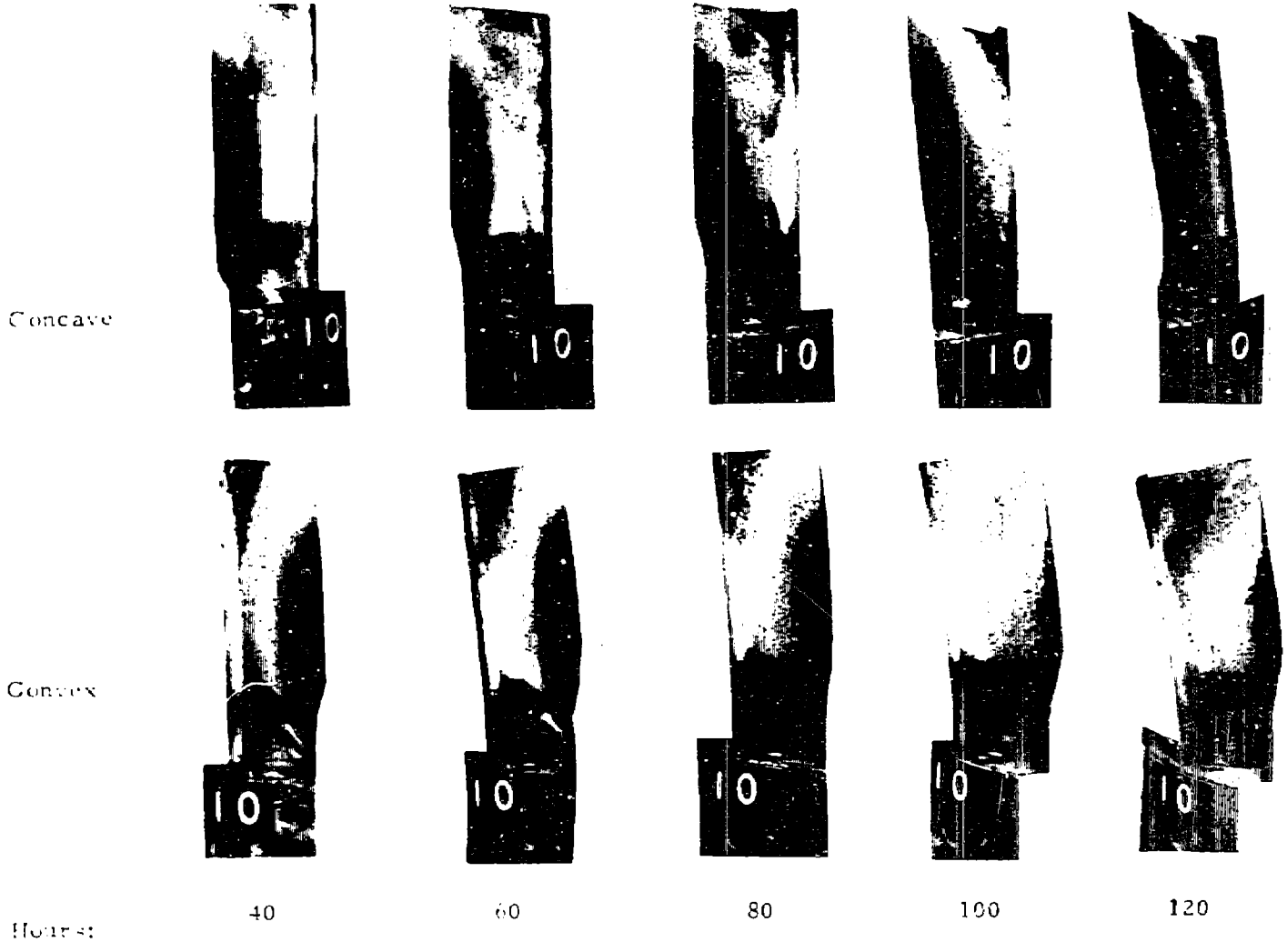

Figure 43. Condition of MAR-M-302 During 120-Hour Test Showing Degradation of SAC Coating.

Leading Edge | Center | Trailing Edge

Etchant: 5 HNO_3, 14 H_2SO_4, 20 HF, 50 H_2O

Mag.: 300X

Figure 44. Relative Degradation of VH 112 Coating on C-3015.

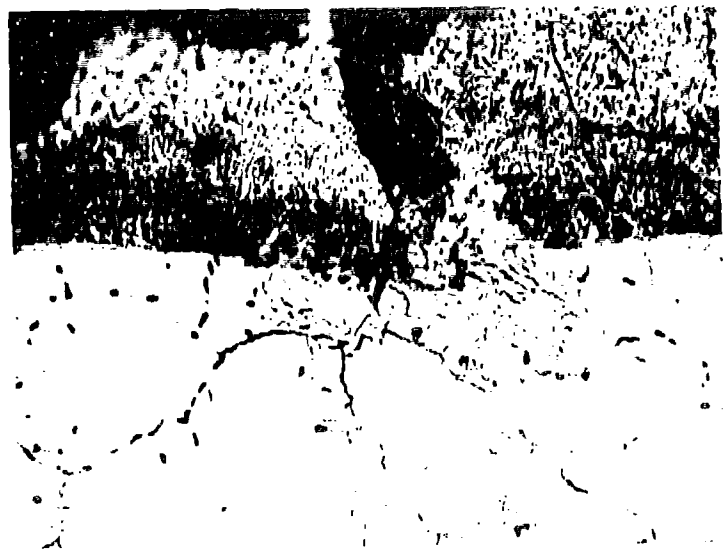

Leading Edge

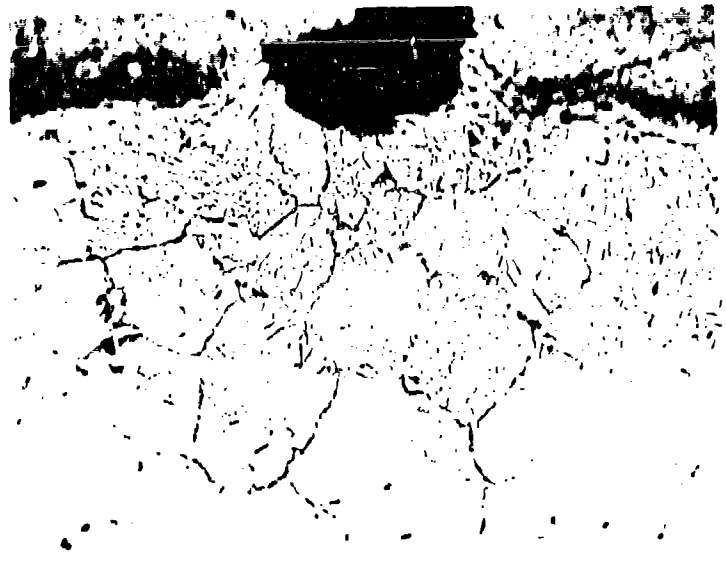

Trailing Edge

Etchant: 5 HNO_3, 14 H_2SO_4, 20 HF, 50 H_2O Mag.: 600X

Figure 45. Substrate Degradation at the Base of Oxidized Cracks on VH112 Coated C-3015.

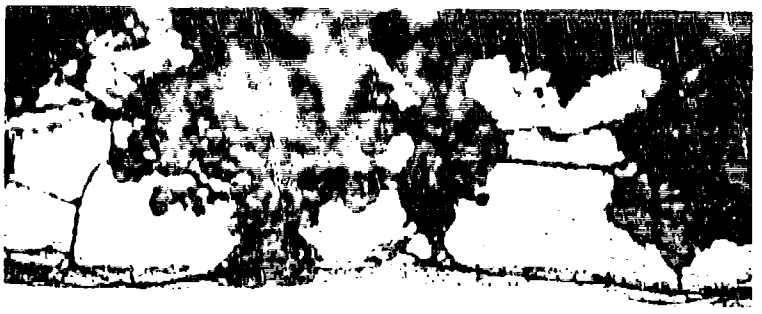

Trailing
Edge

Leading
Edge

Etchant: 5 HNO_3, 14 H_2SO_4, 20 HF, 50 H_2O Mag.: 300X

Figure 46. Degradation of VH 112 Coating on B-66.

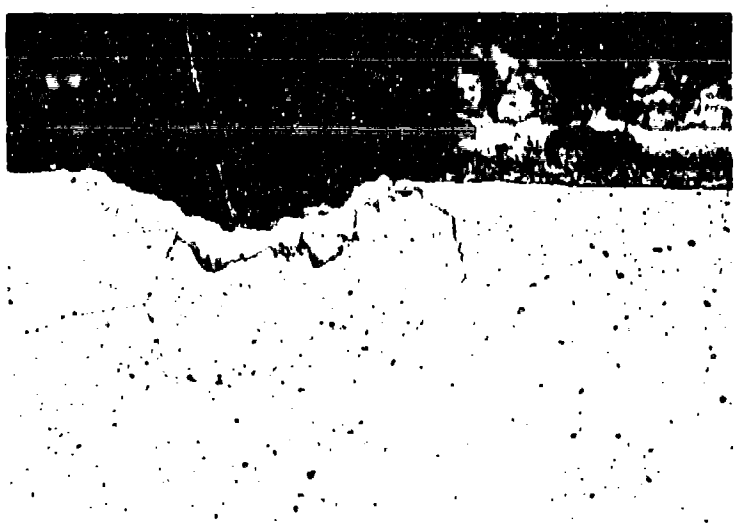

Etchant: 5 HNO_3, 14 H_2SO_4, 20 HF, 50 H_2O Mag.: 600X

Figure 47. Oxidation of Base Metal In Spalled Area of VH-112-Coated B-66.

Mag.: 300X

Mag.: 600X

Etchant: 5 HNO_3, 14 H_2SO_4, 30 HF, 50 H_2O

Figure 48. Degradation of R5[illegible]-Coating on B[illegible]

Etchant: 5 HNO_3, 14 H_2SO_4, 20 HF, 50 H_2O Mag.: 100X

Figure 49. R512E-Coated B-66 Showing Ballistically Impacted Area. Arrow points to intact coating of adjoining area.

Unetched Mag.: 300X

701 Coated/Inco 713C

Etchant: Marbles Mag.: 300X

701 Coated/M3608

Figure 50. Typical Microstructures of Aluminide-Coated Superalloys After Environmental Testing at 2200°F.